MIT Libraries | DSpace@MIT

MIT Open Access Articles

Heterogeneous Responses of Hematopoietic Stem Cells to Inflammatory Stimuli Are Altered with Age

The MIT Faculty has made this article openly available. ***Please share*** how this access benefits you. Your story matters.

Citation: Mann, Mati et al. "Heterogeneous Responses of Hematopoietic Stem Cells to Inflammatory Stimuli Are Altered with Age." Cell Reports 25, 11 (December 2018): 2992–3005 © 2018 The Author(s)

As Published: http://dx.doi.org/10.1016/j.celrep.2018.11.056

Publisher: Elsevier

Persistent URL: https://hdl.handle.net/1721.1/121253

Version: Final published version: final published article, as it appeared in a journal, conference proceedings, or other formally published context

Terms of use: Creative Commons Attribution 4.0 International license

Massachusetts Institute of Technology

Cell Reports

Article

Heterogeneous Responses of Hematopoietic Stem Cells to Inflammatory Stimuli Are Altered with Age

Graphical Abstract

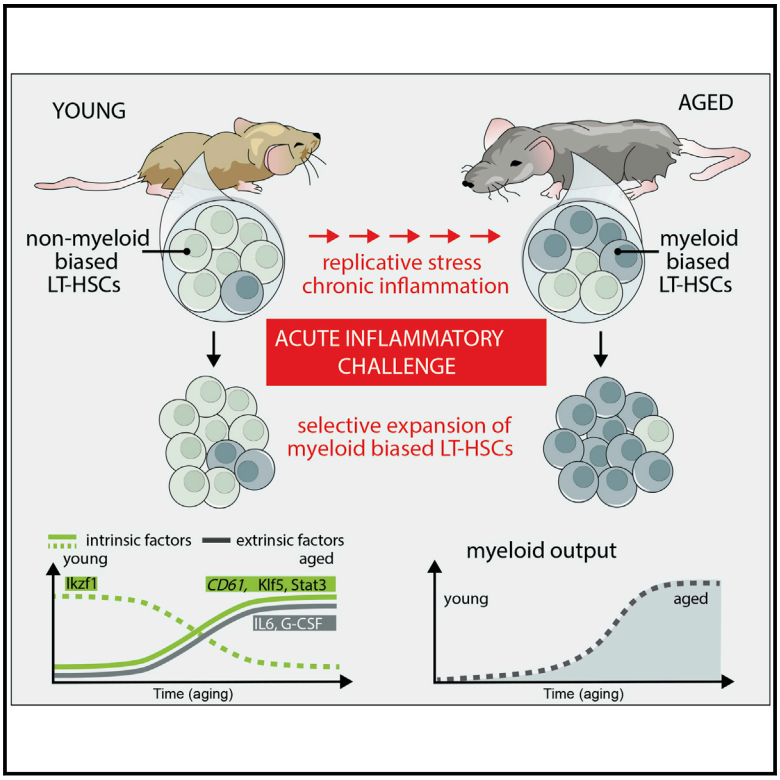

Authors

Mati Mann, Arnav Mehta, Carl G. de Boer, ..., Daneyal Farouq, Aviv Regev, David Baltimore

Correspondence

mati@calech.edu (M.M.), aregev@broadinstitute.org (A.R.), baltimo@caltech.edu (D.B.)

In Brief

Mann et al. show an age-dependent inflammatory response of hematopoietic stem cells (HSCs) and unveil a CD61-high subpopulation primed for inflammatory response. This CD61-high subpopulation is more prevalent in aged mice and has a cell-intrinsic myeloid-biased potential, which is regulated in part by Ikzf1, Klf5, and Stat3 transcription factors.

Highlights

- LT-HSCs from young and aged mice have differential responses to inflammatory challenge
- Aged LT-HSCs demonstrate a cell-intrinsic myeloid bias during inflammatory challenge
- CD61-high surface expression on LT-HSCs marks a myeloid-biased LT-HSC subset
- *Klf5*, *Ikzf1*, and *Stat3* regulate age- and inflammation-related LT-HSC myeloid bias

Mann et al., 2018, Cell Reports *25*, 2992–3005
December 11, 2018 © 2018 The Author(s).
https://doi.org/10.1016/j.celrep.2018.11.056

CellPress

OPEN ACCESS
CellPress

Cell Reports
Article

Heterogeneous Responses of Hematopoietic Stem Cells to Inflammatory Stimuli Are Altered with Age

Mati Mann,[1,5,6,*] Arnav Mehta,[1,2,5] Carl G. de Boer,[3,5] Monika S. Kowalczyk,[3,5] Kevin Lee,[1] Pearce Haldeman,[1] Noga Rogel,[3] Abigail R. Knecht,[3] Daneyal Farouq,[3] Aviv Regev,[3,4,*] and David Baltimore[1,*]
[1]Division of Biology and Biological Engineering, California Institute of Technology, Pasadena, CA 91125, USA
[2]David Geffen School of Medicine, UCLA, Los Angeles, CA 90025, USA
[3]Broad Institute of MIT and Harvard University, Cambridge, MA 02142, USA
[4]Howard Hughes Medical Institute, Koch Institute of Integrative Cancer Biology, Department of Biology, Massachusetts Institute of Technology, Cambridge, MA 02140, USA
[5]These authors contributed equally
[6]Lead Contact
*Correspondence: mati@calech.edu (M.M.), aregev@broadinstitute.org (A.R.), baltimo@caltech.edu (D.B.)
https://doi.org/10.1016/j.celrep.2018.11.056

SUMMARY

Long-term hematopoietic stem cells (LT-HSCs) maintain hematopoietic output throughout an animal's lifespan. However, with age, the balance is disrupted, and LT-HSCs produce a myeloid-biased output, resulting in poor immune responses to infectious challenge and the development of myeloid leukemias. Here, we show that young and aged LT-HSCs respond differently to inflammatory stress, such that aged LT-HSCs produce a cell-intrinsic, myeloid-biased expression program. Using single-cell RNA sequencing (scRNA-seq), we identify a myeloid-biased subset within the LT-HSC population (mLT-HSCs) that is prevalent among aged LT-HSCs. We identify CD61 as a marker of mLT-HSCs and show that CD61-high LT-HSCs are uniquely primed to respond to acute inflammatory challenge. We predict that several transcription factors regulate the mLT-HSCs gene program and show that *Klf5*, *Ikzf1*, and *Stat3* play an important role in age-related inflammatory myeloid bias. We have therefore identified and isolated an LT-HSC subset that regulates myeloid versus lymphoid balance under inflammatory challenge and with age.

INTRODUCTION

Long-term hematopoietic stem cells (LT-HSCs) encounter continued stresses throughout life, yet maintain appropriate immune cell output (Akunuru and Geiger, 2016; Denkinger et al., 2015; Dykstra et al., 2011; Geiger et al., 2013; Morita et al., 2010; Sawai et al., 2016; Yamamoto et al., 2018). These stresses include replicative stress (Bernitz et al., 2016; Flach et al., 2014; Wang et al., 2012) and acute and chronic infectious challenge (King and Goodell, 2011; Nagai et al., 2006). Physiologic aging in both humans and mice leads to permanent changes in LT-HSC function, such as myeloid-biased hematopoietic output, and poor response to infections (Akunuru and Geiger, 2016). This is often accelerated in settings of chronic inflammation and, when dysregulated, can lead to replicative exhaustion and extramedullary hematopoiesis (Esplin et al., 2011; Mehta et al., 2015).

Hematopoietic stem and progenitor cells (HSPCs) express innate immune receptors (King and Goodell, 2011), such as Toll-like receptors (TLRs), and respond to many inflammatory mediators, including interferon gamma (IFN-γ) (Baldridge et al., 2010), macrophage colony-stimulating factor (M-CSF) (Mossadegh-Keller et al., 2013), and the Gram-negative bacterial component lipopolysaccharide (LPS) (Nagai et al., 2006). In response to acute LPS exposure, LT-HSCs increase proliferation, mobilize to the peripheral bloodstream (King and Goodell, 2011), and initiate emergency myelopoiesis to increase the system's output of innate immune cells (Haas et al., 2015). This increased output may also be mediated by hematopoietic progenitors, such as multipotent progenitors (MPPs) (Pietras et al., 2015; Young et al., 2016), in part due to the direct secretion of cytokines that drive myeloid differentiation (Zhao et al., 2014).

Several hypotheses have been proposed to explain the age-related changes in LT-HSC function (Kovtonyuk et al., 2016). First, cell-intrinsic changes within each aged LT-HSC may make it inherently myeloid biased (Grover et al., 2016; Rossi et al., 2005). Second, the LT-HSC population may comprise subsets of myeloid- and lymphoid-biased cells, the composition of which changes with age such that myeloid-biased LT-HSCs are more prevalent within the aged LT-HSC population (Dykstra et al., 2007; Gekas and Graf, 2013; Yamamoto et al., 2013). The true nature of these age-related changes may in fact be a combination of both of these hypotheses, so that with age there is a growing subset of more intrinsically myeloid-biased LT-HSCs.

The transcriptional and functional states of LT-HSCs in steady state and in response to inflammatory mediators may help shed light on these questions, but are still poorly understood.

 © 2018 The Author(s).
This is an open access article under the CC BY license (http://creativecommons.org/licenses/by/4.0/).

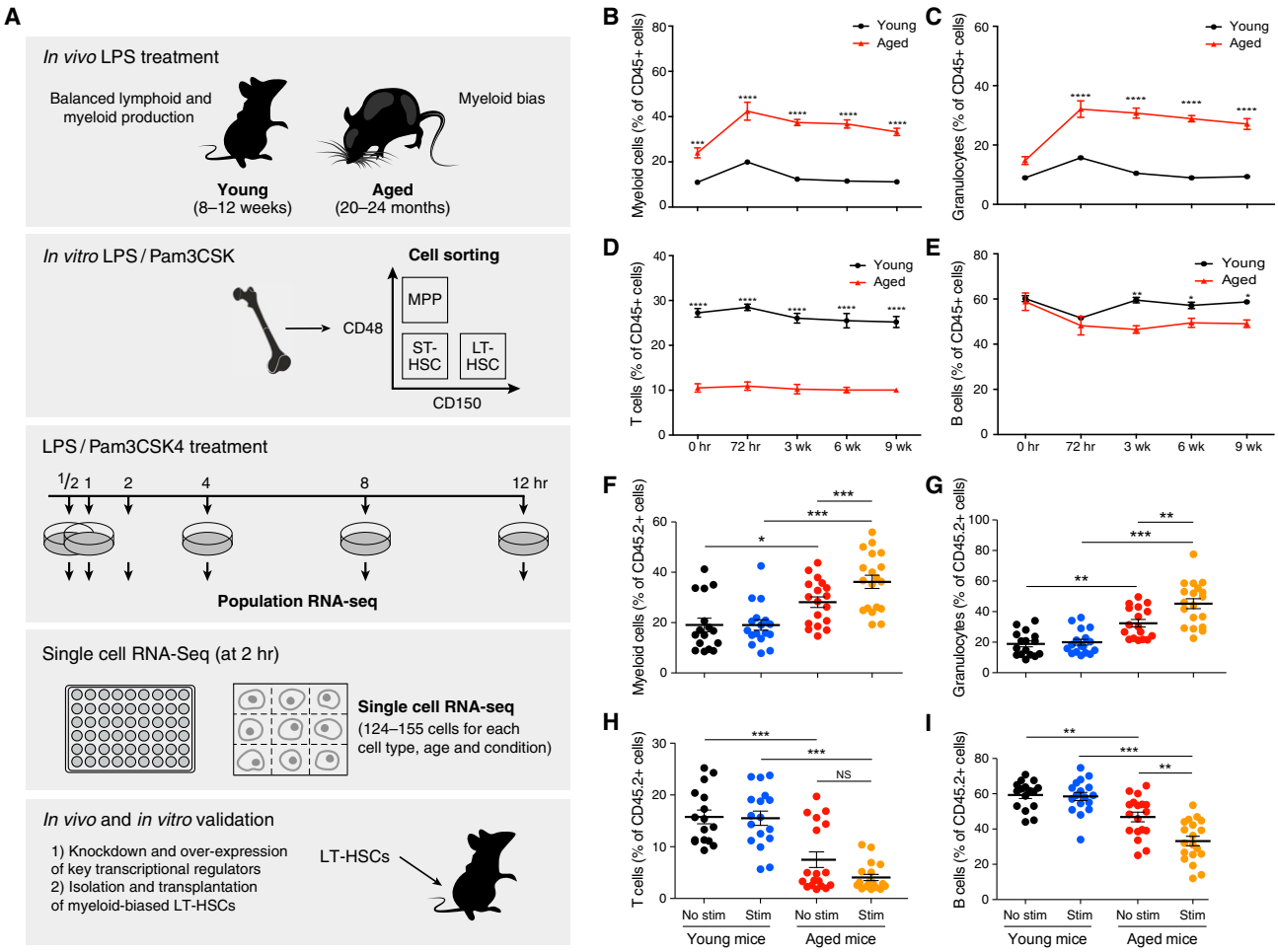

Figure 1. Aged Hematopoietic Stem Cells Exposed to Inflammatory Signals Demonstrate Increased Myeloid Output in a Cell-Intrinsic Manner

(A) Schematic overview of the approach.

(B–E) Young and aged mice were exposed to a second dose of LPS 1 month after the initial LPS challenge and the frequencies of (B) CD11b$^+$, (C) Gr-1$^+$, (D) CD3$^+$, and (E) CD19$^+$ were observed for 9 weeks.

(F)–(I) LT-HSCs sorted from young and aged CD45.2 mice were stimulated with LPS and Pam3csk4 for 2 hr before competitive transplant into CD45.1 recipients. Peripheral blood CD45.2 (F) CD11b$^+$, (G) Gr-1$^+$, (H) CD3$^+$, and (I) CD19$^+$ frequencies were measured by flow cytometry at 3 months post-reconstitution (n = 11–12 per group).

Data represent at least two independent experiments and are presented as means ± SEMs. *$p < 0.05$, **$p < 0.01$, and ***$p < 0.001$. p values were corrected for multiple hypothesis testing by Bonferroni's multiple comparison test.

A number of epigenomic and transcriptomic changes have been observed during bulk and single-cell expression analyses of young and aged LT-HSCs (Cabezas-Wallscheid et al., 2014; Grover et al., 2016; Kowalczyk et al., 2015; Sanjuan-Pla et al., 2013; Sun et al., 2014; Yu et al., 2016). However, it is unclear how these changes lead to altered LT-HSC function, as seen with age-related myeloid bias (Dykstra et al., 2011; Gekas and Graf, 2013; Yamamoto et al., 2018). In particular, a previous study using single-cell RNA sequencing (scRNA-seq) (Kowalczyk et al., 2015) of steady-state, resting LT-HSCs has not identified a subpopulation structure. An understanding of how inflammatory mediators effect the response of LT-HSCs and how this response changes with age may therefore help elucidate the underlying mechanism of age-related myeloid bias. This may further provide insight into age-related pathologies such as improper immune responses to vaccines or infectious challenge and the development of myeloid leukemia.

In this work, we investigate the acute inflammatory response of mouse HSPCs *in vitro* and *in vivo* and how this response may be altered with age (Figure 1A). We show that major HSPCs subtypes respond transcriptionally to inflammatory stimuli and that age-dependent inflammatory myeloid bias is intrinsic to LT-HSCs, based on bone marrow transplant experiments. Using scRNA-seq, we find that the LT-HSC compartment comprises at least two subsets that become apparent upon stimulation. One of these subsets has features that are consistent with myeloid

bias (referred to as mLT-HSCs), with distinct cell-intrinsic responses to inflammatory stimulation. The myeloid-biased subset expresses high levels of the surface marker CD61, can be prospectively isolated and lead to myeloid bias upon reconstitution, and increases dramatically with age. We further identify putative transcriptional regulators of mLT-HSCs and demonstrate the role of these regulators in age-related myeloid bias and differential responses to TLR ligands.

RESULTS

Inflammation in Aged and Young Mice Leads to Differential Increases in Myeloid Output

To investigate the acute inflammatory response of hematopoietic progenitors from mice at different ages, we challenged 8- to 12-week-old ("young") and 20- to 24-month-old ("aged") mice with a single intraperitoneal injection of LPS (0.5 mg/kg; Figures S1A–S1D). We observed a >2-fold increase in peripheral blood myeloid frequencies in aged mice by 72 hr post-challenge, whereas only a minimal increase was seen in young mice (Figures S1A and S1B). These changes in myeloid output returned to baseline frequencies by 9 weeks post-challenge. The baseline frequency of T cells in aged mice was 2-fold lower than in young mice, but both cohorts had increased T cell output 72 hr after LPS challenge (Figure S1C). In contrast, B cell output in both young and aged cohorts decreased after LPS treatment, and the acute response was particularly dramatic in aged mice, which had a 2-fold loss in the frequency of B cells by 72 hr and then recovered to baseline levels by 6 weeks post-challenge (Figure S1D). Aged mice therefore demonstrated a strong acute increase in myeloid output in response to inflammatory challenge that was not observed in young mice.

To evaluate the cumulative effect of acute inflammatory challenges on myeloid output, we performed a second LPS injection in all cohorts 1 month after the initial challenge. This resulted in an upregulation of peripheral blood myeloid cells in aged mice, whereas again, only a milder increase in myeloid output was seen in young mice (Figures 1B and 1C). While myeloid output in young mice returned to baseline within 3 weeks, the myeloid cell frequencies of aged mice mildly decreased 3 weeks post-injection, but remained higher than baseline for at least 9 weeks post-injection (Figures 1B and 1C). T cell levels slightly increased in young mice by 72 hr and did not change in aged mice (Figure 1D). Conversely, B cell output decreased in both aged and young mice by 72 hr, but while young B cells returned to baseline levels, the B cell levels of aged mice remained lower than baseline by 9 weeks post-injection (Figure 1E).

The spleens of stimulated aged mice revealed increased myeloid cell frequencies and a dramatic loss of T cells compared to young mice (Figure S1E). Finally, the bone marrow of stimulated aged mice had a 3-fold enrichment for LT-HSCs compared to stimulated young mice, with a milder enrichment in short-term HSCs (ST-HSCs) and MPPs (Figure S1F). This enrichment in LT-HSCs is higher than the 2-fold enrichment reported between unstimulated aged and young mice (Beerman et al., 2010; Mehta et al., 2015). These results suggest that repeated acute inflammatory stimuli in aged mice enhance myeloid-biased output from HSPCs and that the differences in immune cell output may originate from LT-HSCs.

Inflammation Leads to a Distinctive, Long-Term Myeloid-Biased Output in Aged LT-HSCs

To examine whether inflammation leads to a cell-intrinsic myeloid bias in LT-HSCs, we tested the impact of stimulation on the ability of young and aged LT-HSCs to reconstitute the immune system. Specifically, we first sorted LT-HSCs, ST-HSCs, and MPPs from young and aged CD45.2 C57BL/6 mice. The sorted cells were either maintained unstimulated or stimulated with LPS and Pam3csk4 for 2 hr *in vitro* and subsequently transplanted into lethally irradiated young CD45.1 C57BL/6 mice. Peripheral blood counts of CD45.2-expressing cells were monitored for 4 months (Figures 1F–1I, S2A, and S2B). Both unstimulated and stimulated young and aged LT-HSCs demonstrated long-term reconstitution of the immune system in primary and secondary transplanted mice (Figures S2A–S2D).

At 3 months post-reconstitution (i.e., 3 months after the *in vitro* LPS and Pam3csk4 challenge), inflammatory challenge of young LT-HSCs did not lead to altered peripheral blood myeloid and lymphoid cell frequencies compared to unstimulated controls (Figures 1F–1I). As previously reported (Beerman et al., 2010; Pang et al., 2011), unstimulated aged LT-HSCs had higher peripheral blood myeloid output and lower lymphoid output compared to unstimulated young LT-HSCs (Figures 1F–1I). However, stimulated aged LT-HSCs demonstrated a marked additional increase in the frequency of peripheral blood myeloid cells (Figures 1F and 1G) and a further decrease in the frequency of peripheral blood B cells (Figure 1H). Thus, aged LT-HSCs demonstrated myeloid-biased "memory" of the initial *in vitro* LPS and Pam3csk4 challenge that persisted for several months post-reconstitution, a phenomenon not seen with stimulated young LT-HSCs. No significant difference in LT-HSC frequency was observed between cohorts, including in the previously identified myeloid-biased $CD41^+$ LT-HSC subpopulation (Gekas and Graf, 2013) (Figures S2E–S2H). These results suggest that direct TLR stimulation of aged LT-HSCs leads to a long-term increase in myeloid bias. It is not clear, however, whether this increase is cell intrinsic or due to changes in the composition of the LT-HSC population.

HSPCs Demonstrate a Canonical Transcriptional Response to TLR Ligands

We hypothesized that the differential effects of young and aged stimulated LT-HSCs may be due to a variable transcriptional response to inflammatory signals. To test this hypothesis, we measured the transcriptional profiles of populations of HSPCs from young and aged mice during a 12-hour time course of LPS and Pam3csk4 stimulation *in vitro* (Figure 2A). LT-HSCs, ST-HSCs, and MPPs from both young and aged mice demonstrated a robust and similar transcriptional response to inflammatory stimuli (Figure 2B; Table S1), which largely resembled that seen in mature cell types with different physiological functions such as bone marrow-derived dendritic cells (BMDCs) after LPS stimulation (Figures 2B–2D) (Jovanovic et al., 2015). This response includes the same temporal ordering of induction in inflammatory gene clusters as in mature cell types (Amit et al.,

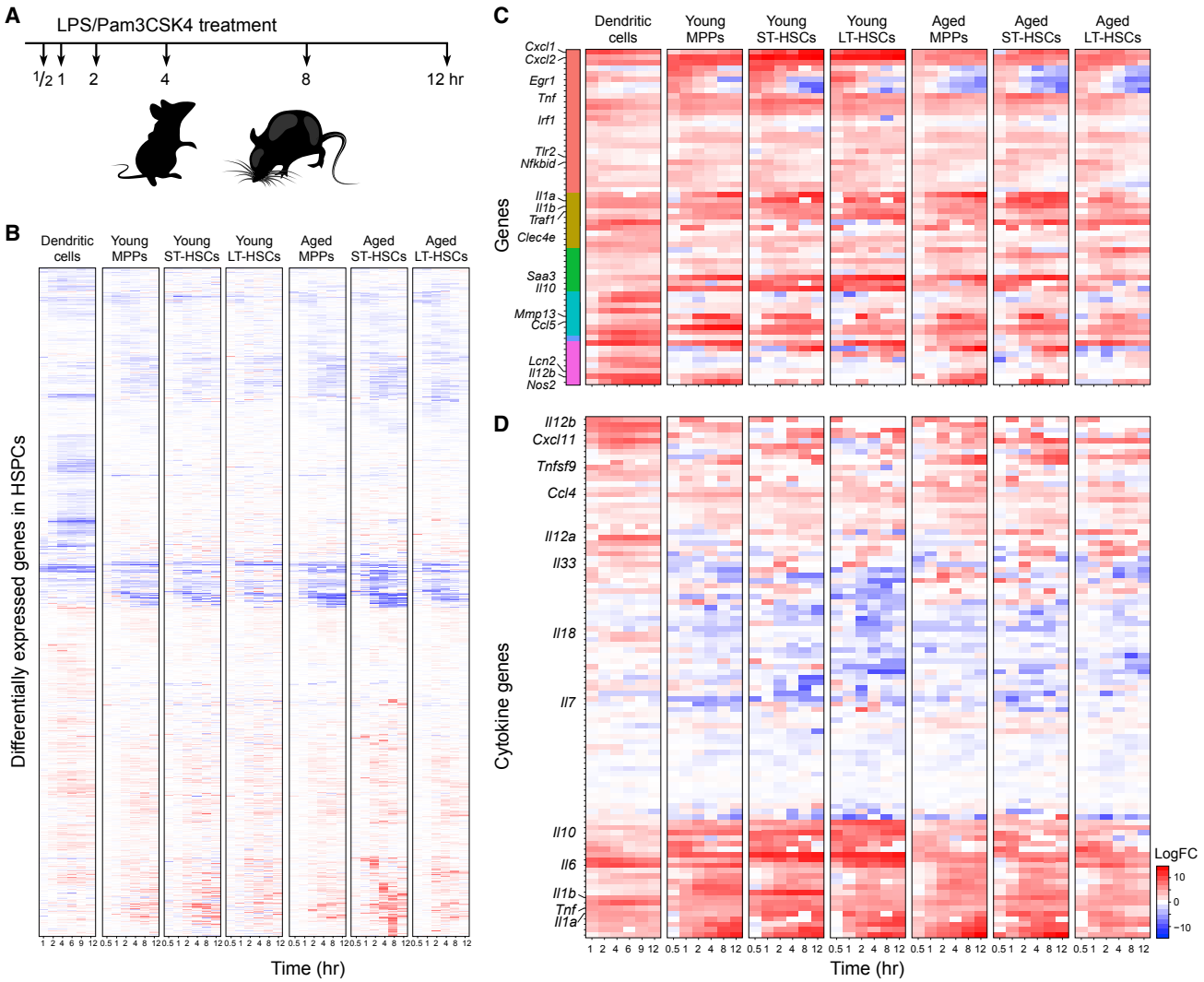

Figure 2. Early Hematopoietic Progenitors Demonstrate a Rapid Transcriptional Response to Inflammatory Signals

(A) Schematic of LPS and Pam3CSK4 time course experiment. LT-HSCs, ST-HSCs, and MPPs from five young and five aged mice were exposed to LPS and Pam3CSK4 *in vitro* for the indicated time, after which RNA was harvested for bulk RNA sequencing.

(B) Heatmap of differentially expressed genes in young and aged hematopoietic progenitors alongside an expression map of mature bone marrow-derived dendritic cells (DCs) challenged with LPS for comparison.

(C) Heatmap of NF-κB-regulated inflammatory genes clustered by temporal expression patterns described previously.

(D) Heatmap of cytokines expressed in early progenitors and DCs.

2009; Ramirez-Carrozzi et al., 2009), upregulation of nuclear factor κB (NF-κB)-related genes (Figure 2C) (Bhatt et al., 2012; Hao and Baltimore, 2009), and induction of the expression of several effector cytokines (Figure 2D), albeit at slightly lower levels (Figures S3A–S3C). Among the differentially expressed genes between all of the cell types, HSPCs from both young and aged mice presented similar patterns compared to BMDCs (Figure 2B; for a complete list of differentially expressed genes and their Gene Ontology [GO] enrichments, see Table S2). Thus, the response of young and aged HSPCs to inflammatory activation resembles the canonical response of mature cells to similar stimulation, both in the identity of the regulated genes and in the timescale of the response. This suggests that the differences in the reconstitution outcome were not simply related to the differences in the transcriptional response when measured at the population level.

scRNA-seq Reveals Two Subsets of LT-HSCs with Distinct Responses to Inflammatory Stimulus

Next, we considered the possibility that there are different subsets of LT-HSCs either in steady state or post-stimulation ("cell-intrinsic changes") and that their relative proportions may change with age ("compositional changes"). Early hematopoietic progenitors comprise heterogeneous functional

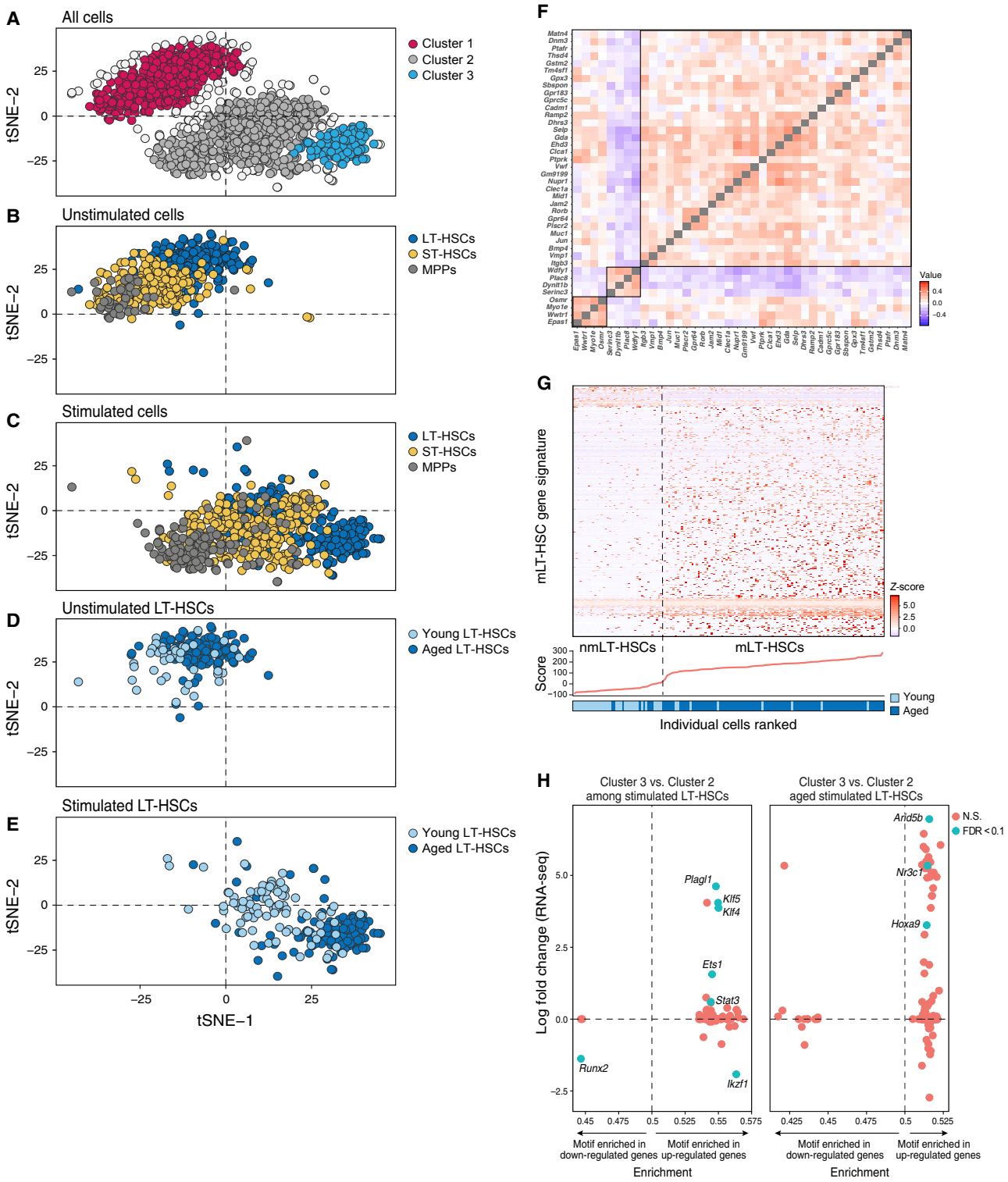

Figure 3. Single-Cell RNA Sequencing Reveals Heterogeneity in the Hematopoietic Stem Cell Compartment that Is Altered with Age

(A–E) LT-HSCs, ST-HSCs, and MPPs from five young and four aged mice were stimulated with LPS and Pam3CSK4 and sorted for single-cell RNA sequencing (scRNA-seq). scRNA-seq data for all cells, projected on two t-distributed stochastic neighbor embedding (t-SNE) axes.

(A) Density-based clusters.

(legend continued on next page)

subpopulations (Benz et al., 2012; Gekas and Graf, 2013; Morita et al., 2010; Sanjuan-Pla et al., 2013), which often reveal themselves in response to inflammatory stimuli (Haas et al., 2015; Zhao et al., 2014). While a previous scRNA-seq study we performed of LT-HSCs has mostly revealed age-related differences in the cell cycle (Kowalczyk et al., 2015), we hypothesized that stimulation could unveil additional cell-intrinsic distinctions that were not observed in resting cells.

To determine the composition of HSPCs in each age group and condition, we performed full-length scRNA-seq (Picelli et al., 2013) of young and aged LT-HSCs, ST-HSCs, and MPPs, with and without 2 hr of *in vitro* LPS and Pam3csk4 stimulation of sorted cells. As we aimed to distinguish cell-intrinsic, possibly subtle, stimulus-specific states within a very-well-defined cell population, we opted for the deeper coverage full-length scRNA-seq approach over massively parallel approaches (Tanay and Regev, 2017; Wagner et al., 2016). We profiled 2,046 individual cells from 9 mice (5 young, 4 aged), with 124–186 cells for each given cell type and condition. To eliminate sources of variability resulting from known confounding factors, we removed 611 cells as being of low quality and 58 as possible contaminants (STAR Methods). In addition, 578 of the cells were actively cycling (STAR Methods). Overall, we retained 949 cells for subsequent analysis, comprising 187 MPPs, 404 ST-HSCs, and 358 LT-HSCs.

We identified 3 major groups of cells using unsupervised clustering (STAR Methods), denoted clusters 1, 2, and 3 (Figure 3A). Cluster 1 (311 cells) contained most (302 of 354) of the unstimulated HSPCs of all types, forming a continuum from MPPs to LT-HSCs (Figure 3B), with aged and young LT-HSCs clustering together (Figure 3D), and hardly any stimulated cells. Clusters 2 (103 cells) and 3 (421 cells) almost exclusively contained stimulated HSPCs (Figure 3C) and had opposing patterns with respect to aged and young LT-HSCs (Figure 3E): cluster 3 contained 77% of the aged stimulated LT-HSCs and only 13% of the young stimulated LT-HSCs, whereas cluster 2 had 72% of the young stimulated LT-HSCs and only 10% of the aged stimulated LT-HSCs (Figure 3E). This suggests that there are distinct subsets of LT-HSCs in the bone marrow that can be discerned by their different cell-intrinsic responses to stimulation and that the relative frequencies of these subsets appear to change with age. Of note, the distinction between these LT-HSC subsets could be discerned only with stimulation, and no significant difference was found within unstimulated or stimulated ST-HSCs or MPPs (Figures S3D and S3E). Given these findings, we focused further analyses on LT-HSCs.

Myeloid-Biased LT-HSCs Can Be Identified by a Distinct Gene Signature under Inflammatory Conditions

To identify the differences between stimulated LT-HSCs in cluster 3 and cluster 2, we examined genes that were differentially expressed between the two clusters. Cluster 3-specific genes were enriched for genes related to myeloid function and inhibiting lymphoid differentiation, including pathways related to NF-κB localization, negative regulation of lymphocyte development, macrophage proliferation, cell migration and localization, and platelet-derived growth factor signaling (Figure S3F). Cluster 2-specific genes were enriched for genes involved in lymphocyte development, cell proliferation, and acute inflammatory response (Figure S3G). Cells in any given cluster, regardless of age, were similar to one another and distinctly different from cells in the other cluster. These data are consistent with a model in which aged and young LT-HSCs have different proportions of cells that display unique lineage-biased pathway preferences in response to inflammatory signals.

To test whether the LT-HSC subsets also exist in unstimulated cells in steady-state conditions, we identified 47 genes that were significantly differentially expressed both when comparing cluster 3 versus cluster 2 (single-cell differential expression [SCDE] [Kharchenko et al., 2014], false discovery rate [FDR] <0.01) and when comparing unstimulated aged versus young LT-HSCs within cluster 1 (Figure S3H; STAR Methods; SCDE FDR <0.1). We then tested whether these 47 genes coherently co-vary across the 149 unstimulated LT-HSCs, and thus may reflect a variable cell state within these cells. We identified three distinct co-varying gene clusters (Figure 3F), two of which contained genes involved in myeloid and platelet differentiation, including *Selp*, *Vwf*, *Gpr64*, *Plscr2*, and *Wdfy1*. Notably, recent studies have reported myeloid-biased CD41, Vwf, or CD150-high expressing LT-HSC subpopulations (Dykstra et al., 2011; Gekas and Graf, 2013; Sanjuan-Pla et al., 2013); in our analysis, aged LT-HSCs have increased yet variable expression of CD150 and Vwf and no significant difference in CD41 expression (Figures S3I–S3K).

Next, we generated a refined gene signature. We first scored unstimulated LT-HSCs with the initial set of 47 genes (Figure S3H), identifying 2 putative cell subsets (STAR Methods). Second, we used these subsets to initialize *k*-means clustering ($k = 2$) within the unstimulated LT-HSCs. We used the identities of the cells based on this clustering to designate them as myeloid-biased LT-HSCs (mLT-HSCs) and non-mLT-HSCs (nmLT-HSCs). We tested these 2 final clusters for differentially expressed genes, finding 365 upregulated genes and 34 downregulated genes in the mLT-HSC cluster, which we used to

(B–E) Single-cell t-SNE plots (as before) indicating all cell types among (B) unstimulated and (C) stimulated cells, and mouse ages among (D) unstimulated and (E) stimulated LT-HSCs.

(F) Correlation across cells between DE genes common to both simulated cluster 3 versus cluster 2 and unstimulated aged versus young LT-HSCs. Three clusters of correlated genes are identified.

(G) Heatmap represents the expression values of genes in the unstimulated myeloid-biased gene signature for each single unstimulated LT-HSC. The panels at bottom show the myeloid signature score for each cell and is the basis for the ordering of the x axis. The bottom color-coded bar shows the age of the animals from which the cells were derived.

(H) Enrichment of transcription factor motifs in enhancers of cluster 3- versus cluster 2-specific genes for all cells (left), or only aged LT-HSCs (right) (x axis) and differential expression of the transcription factor (TF) genes themselves in the same comparison (y axis). Significant genes (FDR <0.1) are indicated. An enrichment score >0.5 indicates that the TF motif is enriched among genes that are expressed more highly in cluster 3, while a score <0.5 indicates that the TF is expressed more highly in cluster 2.

define our mLT-HSC signature (SCDE FDR <0.1 and the same direction of change as for stimulated mLT-HSCs) (Table S3).

In the final *k*-means clusters, 92% of cells in the myeloid-biased cluster were aged cells and only 8% were young cells (Figure 3G, right of the dashed line), while only 20% of cells in the non-myeloid-biased cluster were aged cells and 80% were young cells (Figure 3G, left of the dashed line). This is consistent with our finding that the frequency of stimulated mLT-HSCs increases with age (Figure 3E). Applying the same signature to our stimulated LT-HSCs or to an independent dataset of unstimulated aged and young LT-HSCs from two mouse strains (Kowalczyk et al., 2015) showed consistent results; while the LT-HSC population is inherently heterogeneous, more aged LT-HSCs score highly for the mLT-HSC signature (Figures S3L and S3M). Thus, the mLT-HSC signature allowed us to identify the subtle portion of myeloid-biased-like cells among the young unstimulated LT-HSCs and to show that the proportion of high-scoring mLT-HSC cells increases with age.

Klf5, Ikzf1, and Stat3 Regulate Age-Related Inflammatory Myeloid Bias of LT-HSCs

To identify transcription factors (TFs) that may regulate differentially expressed genes between the mLT-HSC and nmLT-HSC subsets, we looked for enriched TF motifs in the enhancer sequences associated with these genes (Lara-Astiaso et al., 2014) (Figure 3H). In particular, we focused on TFs that themselves were differentially expressed between mLT-HSCs and nmLT-HSCs, because altered transcriptional regulation of a TF may affect its target genes. Among the nine significant TFs whose motifs were enriched in enhancers of differentially expressed genes were *HoxA9*, *Klf4*, *Klf5*, *Ikzf1*, and *Stat3*, which we chose to further test given their known putative roles in HSPC biology (Figure 3H, blue dots).

To test the role of these TFs in age-related myeloid bias, we transplanted young or aged HSPCs with short hairpin RNA (shRNA) knockdowns of each TF into young irradiated C57BL/6 recipient mice (Figure S4A). Of the tested TFs in steady state, *Klf5*, *Ikzf1*, and *Stat3* had significant, age-dependent effects, whereas *HoxA9* and *Klf4* did not (Figures S4B–S4E). Consistent with the upregulated expression of *Klf5* in mLT-HSCs, we found that knock down of *Klf5* in aged LT-HSCs resulted in increased lymphoid output (Figure S4C) and decreased myeloid output to levels seen with control young LT-HSCs (Figures S4D and S4E). There was no immediately apparent effect of *Klf5* knockdown in young LT-HSCs. Knock down of *Ikzf1* in young LT-HSCs resulted in decreased lymphoid output (Figure S4C). Knockdown of *Ikzf1* in aged LT-HSCs had no significant effect on lymphoid output, but like knock down of *Klf5*, it resulted in decreased myeloid output to levels seen with control young LT-HSCs (Figures S4D and S4E).

We next tested whether these TFs regulate the myeloid output of LT-HSCs under conditions of inflammatory stress. To do this, we challenged the aforementioned shRNA knockdown mice with LPS (as in Figures 1B–1E). As expected, after the LPS challenge, mice transplanted with control aged LT-HSCs showed a sustained upregulation of myeloid output during the 3 weeks (Figures 4A–4C, solid red lines), whereas mice transplanted with control young HSPCs had only a transient increase in myeloid output, followed by rapid recovery to baseline (Figures 4A–4C, solid black lines). The response to LPS of mice transplanted with aged HSPCs expressing *Klf5*, *Ikzf1*, or *Stat3* shRNAs phenocopied that of mice transplanted with control young HSPCs (Figures 4A–4C and S4F–S4H, dashed red lines). Thus, *Klf5*, *Ikzf1*, and *Stat3* may play a critical role in regulating inflammatory myeloid bias in aged LT-HSCs. No dysregulation in immune output was seen in mice transplanted with HSPCs expressing *HoxA9*, *Klf4*, or *Zbtb4* shRNAs (data not shown).

To identify the cell types that are responsible for the changes observed after *Ikzf1*, *Stat3*, or *Klf5* knockdown in aged HSPCs, we analyzed the bone marrow compartment of all of the mice 3 months post-transplantation. Mice transplanted with aged control cells had higher LT-HSC and common myeloid progenitor (CMP) frequencies and lower common lymphoid progenitor (CLP) frequencies, but no changes in other early progenitor populations when compared to mice reconstituted with young control cells (Figures 4D–4F and S4I–S4K). Knock down of either *Klf5*, *Ikzf1*, or *Stat3* in transplanted aged HSPCs resulted in a decreased frequency of LT-HSCs compared to control aged HSPCs (Figure 4D). We observed no significant effect on the frequency of LT-HSC in the bone marrow in mice transplanted with young HSPCs expressing any of these knockdown constructs (Figure 4D, gray bars) or in aged HSPC transplanted mice expressing *HoxA9* or *Klf4* shRNAs (data not shown). These data therefore suggest that *Klf5*, *Ikzf1*, and *Stat3* may regulate inflammatory myeloid bias in aged LT-HSCs and may do so by altering the function and frequency of LT-HSCs in the bone marrow compartment.

To investigate whether the expression of *Ikzf1, Stat3*, and *Klf5* is sufficient to skew the LT-HSC output, we overexpressed these genes in young and aged HSPCs and transplanted these cells into young irradiated C57BL/6 mice (STAR Methods). *Ikzf1* and *Klf5* overexpression (OE) led to an increase in myeloid output and a decrease in lymphoid output at 3 months post-reconstitution with both young and aged HSPC donor cells (Figures 4G–4I and S5A–S5C). A significant increase in myeloid output was observed after a single LPS injection in *Ikzf1* and *Klf5* OE mice compared to age-appropriate controls. Conversely, *Stat3* OE in both young and aged donor HSPCs yielded comparable myeloid output, which resembled that of aged control mice following LPS injection (Figures 4G–4I and S5A–S5C, dashed lines). Analysis of the bone marrow compartment of *Klf5* OE mice revealed a marked increase in the frequency of LT-HSCs, but no differences in the frequency of ST-HSCs or MPPs. *Klf5* OE did affect downstream progenitors, yielding a higher frequency of bone marrow CMPs and granulocyte macrophage progenitors (GMPs), and a decrease in the frequency of CLPs in both young and aged donors compared to age-matched controls (Figures 4J–4L and S5D–S5H). Similarly, *Ikzf1* OE in both young and aged mice resulted in an increase in bone marrow LT-HSC frequency and a decrease in CLP and lymphoid-primed multipotent progenitor (LMPP) frequencies. *Stat3* OE did not significantly alter LT-HSC frequencies in young or aged mice (Figures 4J–4L and S5D–S5H). These data therefore suggest that *Klf5, Ikzf1*, and *Stat3* may be necessary and sufficient to promote inflammatory myeloid bias.

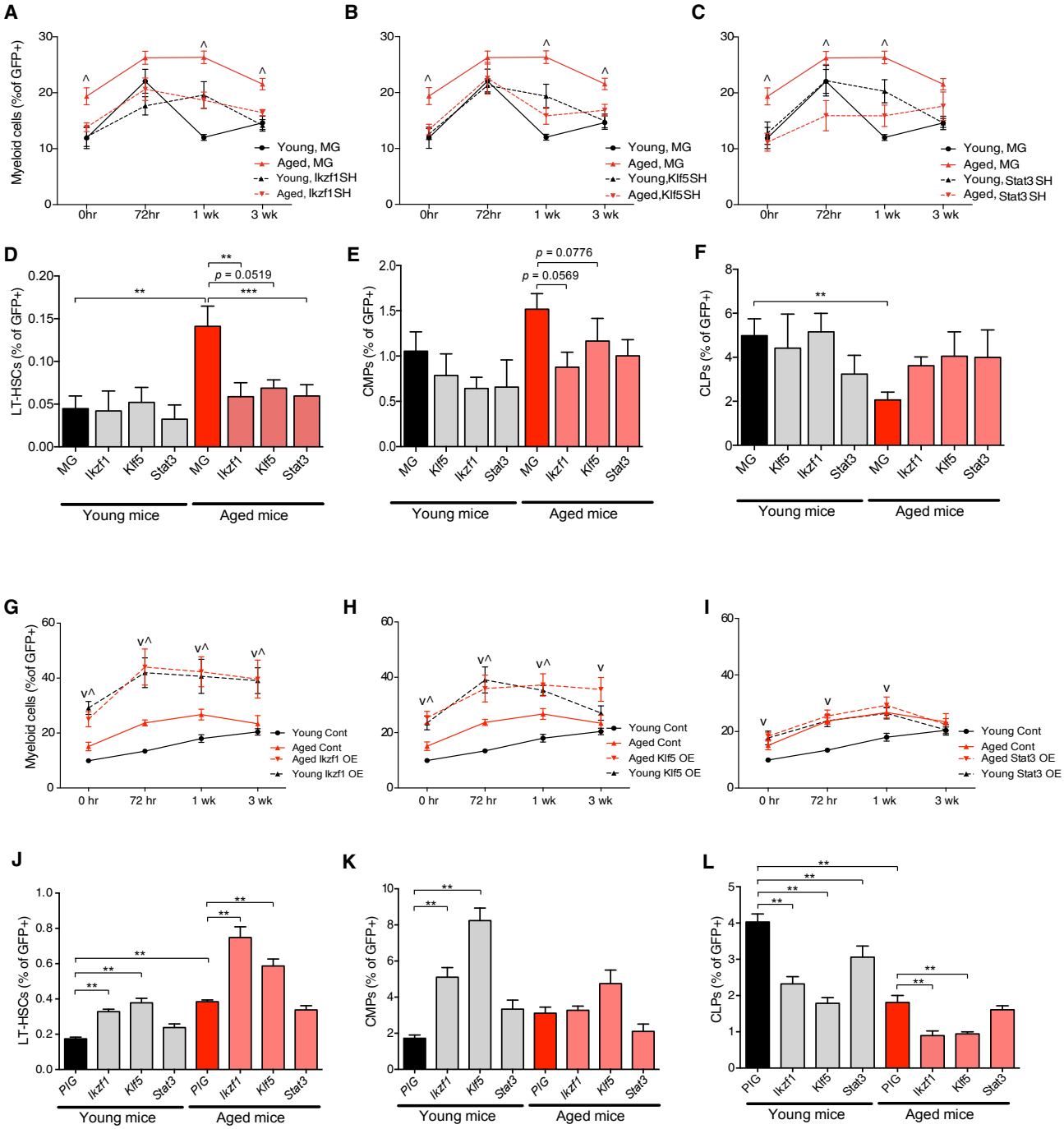

Figure 4. Klf5, Ikzf1, and Stat3 Regulate Steady-State and Inflammatory Age-Related Myeloid Bias

Bone marrow cells from young and aged C57BL/6 mice were transduced with constructs to either knock down (denoted SH in A–F) or overexpress (denoted OE in G–L) the indicated transcription factors. These cells were subsequently reconstituted into lethally irradiated young C57BL/6 recipient mice. These mice were subsequently challenged with a single sublethal dose of LPS, and peripheral blood immune cells were tracked over time by flow cytometry. Shown are peripheral blood myeloid cells for mice with knock down or overexpression of (A) and (G) Ikzf1, (B) and (H) Klf5, and (C) and (I) Stat3. These mice were subsequently harvested, and the bone marrow was analyzed for the frequency of (D) and (J) LT-HSCs, (E) and (K) CMPs, and (F) and (L) CLPs from knockdown and overexpression mice, respectively.

Data represent at least two independent experiments (n = 8–10 mice per group) and are presented as means ± SEMs. In (A)–(C), (G), and (H), ^ denotes $p < 0.05$ for aged shRNA or OE versus aged MG, v denotes $p < 0.05$ for aged shRNA or OE versus young MG using two-way ANOVA. In (D)–(F) and (J)–(L), *$p < 0.05$, **$p < 0.01$, and ***$p < 0.001$. p values were corrected for multiple hypothesis testing by Bonferroni's method.

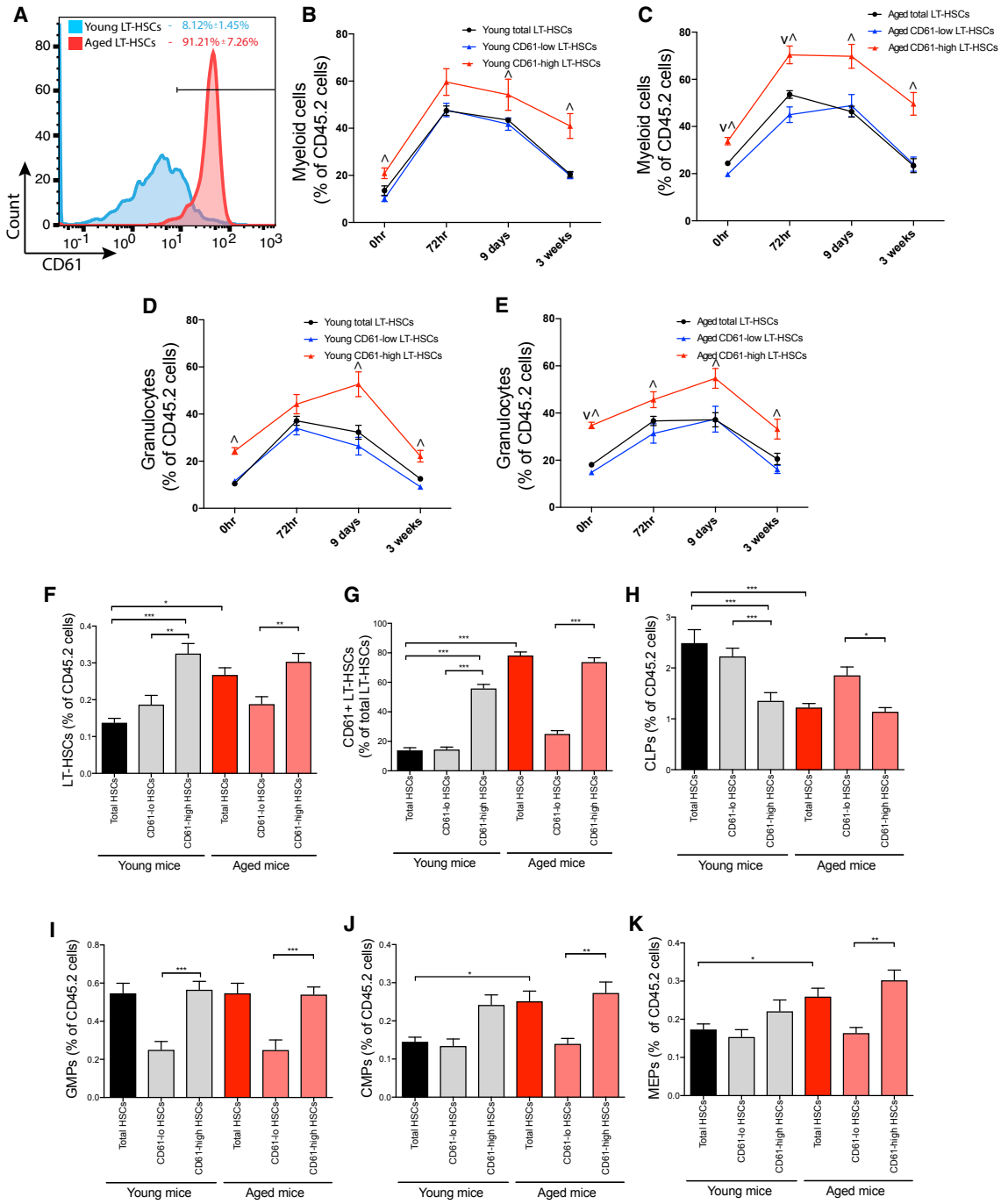

Figure 5. CD61 Expression on LT-HSCs Is a Marker for mLT-HSCs

(A) Flow cytometry plots showing CD61 expression in aged and young LT-HSCs.

(B–E) Total LT-HSCs and those with elevated (CD61-high) and decreased (CD61-low) expression of CD61 from aged and young mice were transplanted into lethally irradiated young C57BL/6 recipient mice. Mice were subsequently challenged with a single dose of LPS, as in Figure 1. Shown are the peripheral blood CD11b$^+$ cell frequencies from mice transplanted with (B) young and (C) aged donor LT-HSCs, and the peripheral blood Gr-1$^+$ frequencies from mice transplanted with (D) young and (E) aged donor LT-HSCs.

(F–K) Transplanted mice were harvested at 4 months post-reconstitution. Shown are the bone marrow frequencies of (F) LT-HSCs, (G) CD61$^+$ LT-HSCs, (H) CLPs, (I) GMPs, (J) CMPs, and (K) MEPs in these mice.

(legend continued on next page)

CD61 Is a Marker for mLT-HSCs

To identify putative surface markers that may characterize mLT-HSCs, we searched the set of genes that were differentially expressed between mLT-HSCs and nmLT-HSCs for those encoding surface proteins that also have a commercially available antibody (Figure S6A; Table S4). Among the surface proteins whose gene expression was elevated in mLT-HSCs compared to nmLT-HSCs were CD61 (Itgb3), CD62p, CD166, CD38, and CD34 (Figure S6A). We tested the surface expression of five of these proteins in aged and young LT-HSCs using flow cytometry (Figures 5A and S6B) and identified CD61 as the most differentially expressed surface protein between the two populations (Figure 5A). The relative proportion of high CD61 expressing LT-HSCs (CD61-high LT-HSCs) and low CD61 expressing LT-HSCs (CD61-low LT-HSCs) was consistent with the proportions of mLT-HSCs and nmLT-HSCs, respectively, as identified in aged and young mice (Figures S6C and S6D). CD61 encodes for β3 integrin. In hematopoietic cells, CD61 has been shown to heterodimerize with α_V/CD51, α_5/CD49e, and α_{IIB}/CD41 to form $\alpha_V\beta_3$, $\alpha_5\beta_3$, or the platelet-specific $\alpha_{IIB}\beta_3$integrins, respectively (Nemeth et al., 2007; Shattil et al., 1998). Using flow cytometry, we found that on LT-HSCs CD51 expression levels correlate most to that of CD61, while CD49e and CD41 expression was only partially correlated with CD61 (Figures S2F, S2H, and S6E–S6G).

We next tested whether CD61-high LT-HSCs are functionally myeloid biased. We sorted CD45.2 CD61-high and CD61-low LT-HSCs (Figures S6C and S6D) from both young and aged mice and transplanted them into young lethally irradiated CD45.1 C57BL/6 mice. At 3 months post-reconstitution, the peripheral blood from mice transplanted with either young or aged CD61-high LT-HSCs had decreased T cell and B cell output and increased myeloid and granulocyte output (Figures S7A–S7D), compared to mice transplanted with young CD61-low cells. To test whether CD61-high LT-HSCs are more prone to inflammatory myeloid bias, we challenged these transplanted mice with LPS. Mice transplanted with both young and aged CD61-high LT-HSCs had a more pronounced and sustained increase in peripheral blood myeloid and a decrease in lymphoid output 3 weeks post-challenge when compared to mice transplanted with total LT-HSCs and CD61-low LT-HSCs of comparable age (Figures 5B–5E and S7E–S7H).

To investigate the cellular basis of myeloid bias with the transplant of CD61-high LT-HSCs, we harvested bone marrow from all of the transplanted mice and analyzed for early hematopoietic progenitors. The bone marrow of mice that had received CD61-high LT-HSCs, whether young or aged, had increased frequencies of LT-HSCs (Figure 5F), the majority of which were CD61-high LT-HSCs compared to mice transplanted with CD61-low LT-HSCs (Figure 5G; 56% and 74% of total LT-HSCs in mice transplanted with young and aged CD61-high LT-HSCs, respectively). The frequency of CD61-high LT-HSCs in mice transplanted with either young or aged CD61-low LT-HSCs was similar to that in mice transplanted with total LT-HSCs of young mice, and >3-fold lower than that of mice transplanted with CD61-high LT-HSCs or total aged LT-HSC mice (Figure 5G). This suggests that CD61-low LT-HSCs may have the potential to convert to a CD61-high LT-HSC phenotype. Consistent with their myeloid-biased phenotype, mice transplanted with CD61-high LT-HSCs had decreased bone marrow CLPs (Figure 5H) and increased GMPs, CMPs, and megakaryocyte-erythrocyte progenitors (MEPs) (Figures 5I–5K) compared to mice transplanted with CD61-low LT-HSCs, regardless of age.

DISCUSSION

In this work, we demonstrate that LT-HSCs have a heterogeneous response to inflammatory stimuli that is altered with age. We show that even the most multipotent of HSPCs directly respond *in vitro* to TLR ligands with a potent transcriptional response. Using scRNA-seq, we demonstrate that both the young and aged LT-HSC compartments comprise at least two distinct subsets of cells with a defined molecular signature. We identify CD61 as a marker of inflammation-responsive mLT-HSCs. We posit that an increased proportion of mLT-HSCs in the bone marrow is a key driver of myelopoiesis and further identify several TFs that regulate steady state and inflammatory myeloid bias in aged LT-HSCs. Our data suggest a revised model (Figure 6) of how inflammation affects LT-HSC function and composition with age.

We show that various types of HPSCs respond transcriptionally to TLR ligands *in vitro* in a similar way to that seen in BMDCs after LPS stimulation (Ramirez-Carrozzi et al., 2009). Given the different functional roles of HSPCs and mature immune cells, this similarity in transcriptional response is surprising. It has been suggested that, as in mature cell types, inducing the expression of NF-κB with LPS and Pam3csk4 in HSPCs may affect cytokine secretion and proliferation (Zhao et al., 2011, 2014). We observed that the dynamics of expression of NF-κB-driven genes was largely similar between HSPCs and BMDCs. Thus, the majority of NF-κB-responsive genes appears to be regulated similarly in both HSPCs and mature cells.

While it has been demonstrated that TLR stimulation of LT-HSCs induces their proliferation (Zhao et al., 2013), our results suggest that it does not alter their long-term reconstitution potential. Aged LT-HSCs maintained a memory of the *in vitro* inflammatory challenge and had increased myeloid output 3 months after transplant compared to unstimulated aged LT-HSCs. These data therefore confirm that LT-HSCs directly sense TLR ligands (Nagai et al., 2006), and in response to this, the aged LT-HSC population has an amplified cell-intrinsic myeloid bias. In the context of physiologic aging, it may be that the accumulation of inflammatory challenges during the lifetime of an animal results in selection and expansion of mLT-HSCs, partially due to direct sensing of these inflammatory signals by these cells.

(A) CD61-high frequencies and SD are depicted for aged (red) and young (blue) (n = 4 per group).
(B–K) Data represent at least two independent experiments (n = 7–12 per group) and are presented as means ± SEMs. ^ denotes $p < 0.05$ for CD61-high versus control, v denotes $p < 0.05$ for CD61-low versus control using two-way ANOVA. *$p < 0.05$, **$p < 0.01$, and ***$p < 0.001$. p values were corrected for multiple hypothesis testing by Bonferroni's method.

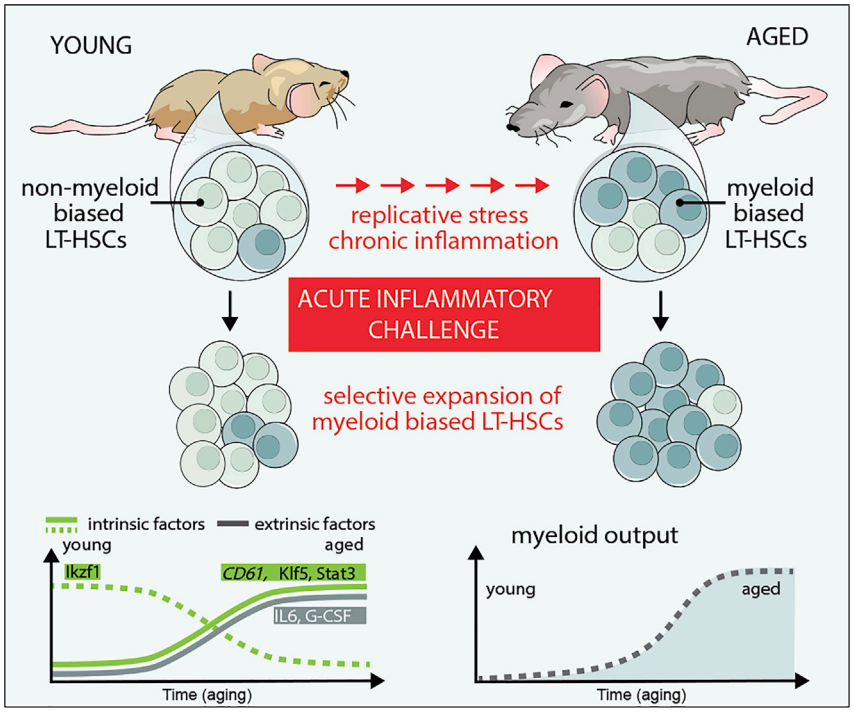

Figure 6. Model of LT-HSC Aging and Inflammatory Myeloid Bias

Shifts in clonal heterogeneity during LT-HSC aging affects the inflammatory response of LT-HSCs. The LT-HSC compartment comprises unbiased and myeloid-biased LT-HSCs. With age, the clonal distribution of LT-HSCs shifts toward myeloid-biased variants, which express high levels of CD61. During acute inflammatory challenges, aged myeloid-biased LT-HSCs preferentially expand, leading to increased myeloid output. Several cell-intrinsic factors, including the transcriptional regulators Klf5, Ikzf1, and Stat3, may play a role in establishing a myeloid-biased differentiation program during aging and inflammation. Extrinsic factors, including inflammatory cytokines and growth factors secreted from other cell types, may also play a role.

mLT-HSC enrichment in turn leads to myeloid bias, further amplifying chronic inflammation and forming a positive feedback loop generating the expansion of mLT-HSCs. This hypothesis is supported by the fact that chronic inflammatory stimulation of young mice, either by repeated LPS challenge or another form of NF-κκB activation, leads to myeloid-biased output (Esplin et al., 2011; Zhao et al., 2013). In addition, human chronic inflammatory diseases such as rheumatoid arthritis in relatively young individuals present with functional changes in HSPCs and a myeloid bias, mirroring aged individuals (Wunder and Henon, 2012; Colmegna et al., 2008). Given that the LT-HSC population is heterogeneous, it has yet to be determined whether inflammation plays a role in either expanding the number of cells in the mLT-HSC state or changing the state of nmLT-HSCs to an mLT-HSC-like state over time.

Using scRNA-seq, we identified subsets within the LT-HSCs population, with distinct transcriptional responses to inflammatory signals. Previous efforts have identified phenotypic markers for megakaryocyte- and mLT-HSC subpopulations (Dykstra et al., 2011; Gekas and Graf, 2013). The gene signature in this study provides functional insight into the basis of myeloid bias in the context of aging and inflammation. Using this gene signature from stimulated LT-HSCs, we uncovered a subset of mLT-HSC-like cells enriched in the unstimulated aged LT-HSC compartment that have the potential to respond uniquely to acute inflammatory signals. This is consistent with recent results suggesting that there is an epigenetically primed subset of LT-HSCs that is uniquely poised to respond to LPS (Yu et al., 2016). We show here that such a subset may also be identified using mRNA expression data.

We identified CD61 as a functional surface marker for mLT-HSCs. CD61-high LT-HSCs from both young and aged mice led to myeloid bias in transplantation experiments, confirming it as a phenotypic marker for mLT-HSCs. CD61 is the β3 integrin subunit, which dimerizes with ItgaV (CD51) to form the vitronectin receptor Itgb3aV, predominantly expressed on macrophages, osteoclasts, dendritic cells, and platelets. CD61 expression has been shown to contribute to the repopulating efficiency of LT-HSC (Umemoto et al., 2008), quiescence (Umemoto et al., 2006), and proliferation (Khurana et al., 2016). Consistent with this, we see that reconstitution efficiency in CD61-low LT-HSCs from both young and aged mice is hampered compared to CD61-high and total LT-HSCs (Figure S7I). Our transplantation experiments with purified CD61-low and CD61-high LT-HSCs resulted in a distribution of CD61 expression in LT-HSCs resembling young and aged total LT-HSC transplants, respectively. This suggests that there may be plasticity between mLT-HSC and nmLT-HSC subpopulations, and it supports the hypothesis that the composition of intrinsically mLT-HSCs changes with age. While we show that CD61 can be used as a phenotypic marker, whether it has a functional role in the formation of mLT-HSCs has yet to be determined.

We additionally identified several transcriptional regulators of inflammatory myelopoiesis in aged stimulated mLT-HSCs. Among these was *Klf5*, which is required for embryonic stem cell self-renewal (Jiang et al., 2008). The enrichment of *Klf5* in mLT-HSCs may therefore play a role in the increased symmetric self-renewal divisions seen in aged LT-HSCs (Geiger et al., 2013; Sudo et al., 2000). Knock down of *Klf5*in aged LT-HSCs, but not in young LT-HSCs, results in decreased myeloid output and decreased LT-HSC bone marrow frequency, while overexpression leads to the opposite effect. Consistent with these results, it has recently been shown that deficiency of *Klf5* in LT-HSCs leads to decreased bone marrow homing of these cells in transplant experiments and reduced output of myeloid cells, especially neutrophils (Shahrin et al., 2016; Taniguchi Ishikawa et al., 2013).

The role of *Ikzf1* in LT-HSC function is less well understood. Previous studies have suggested that *Ikzf1* does not play a role in the myeloid versus the lymphoid lineage commitment of young LT-HSCs (Ng et al., 2009). Our results suggest that in the context

of inflammation, *Ikzf1* may indeed have a positive role in myeloid fate decisions. We found that any perturbation of *Ikzf1* expression levels affects the differentiation potential of LT-HSCs. Consistent with this, *Ikzf1* has been shown to bind enhancer elements of both myeloid and lymphoid genes in human HSPCs (Novershtern et al., 2011). Knock down of *Stat3* in aged LT-HSCs also severely hampered myeloid output after inflammatory challenge. This is consistent with the role of *Stat3* as a major inflammatory TF. In particular, some studies suggest that *Stat3* is induced in response to TLR4 signaling in certain cell types (Kortylewski et al., 2009). Complete knock out of *Stat3* in LT-HSCs has been shown to result in a premature aging phenotype (Mantel et al., 2012); our results suggest that partial loss of *Stat3* is not enough to recapitulate this phenotype.

In summary, our analysis has uncovered mLT-HSCs; identified CD61, a previously unreported marker for inflammation-responsive mLT-HSCs; and revealed three TFs—*Klf5*, *Ikzf1*, and *Stat3*—as important regulators of inflammatory myeloid bias. Since altering the expression of these TFs can alter the balance of myeloid and lymphoid cells during emergency myelopoiesis, manipulating them or other aspects of the unstimulated or stimulated mLT-HSC programs may provide new therapeutic avenues for re-establishing appropriate lymphoid versus myeloid balance to improve immune function and prevent myeloid leukemias with age.

STAR★METHODS

Detailed methods are provided in the online version of this paper and include the following:

- KEY RESOURCES TABLE
- CONTACT FOR REAGENT AND RESOURCE SHARING
- EXPERIMENTAL MODEL AND SUBJECT DETAILS
  - Mice
- METHOD DETAILS
  - Flow cytometry
  - Cell culture
  - Bone marrow transplant experiments
  - *In vivo* LPS challenge
  - Bulk RNA-seq
  - scRNA-seq
  - DNA constructs
  - Virus production
- QUANTIFICATION AND STATISTICAL ANALYSIS
  - Bulk RNA-seq analysis
  - Single cell RNA-seq analysis
  - Single-cell differential expression and gene signatures
  - Stimulated mLT-HSC signature
  - Unstimulated mLT-HSC signature
  - TF motif analysis
  - Statistical tests
- DATA AND SOFTWARE AVAILABILITY

SUPPLEMENTAL INFORMATION

Supplemental Information includes eight figures and five tables and can be found with this article online at https://doi.org/10.1016/j.celrep.2018.11.056.

ACKNOWLEDGMENTS

This work was supported by the Sackler Foundation (D.B.), the Howard Hughes Medical Institute (A.R.), the Klaman Cell Observatory at the Broad Institute (A.R.), the Human Frontiers Science Foundation (M.M.), the National Research Service Award (CA183220, to A.M.), the UCLA/Caltech Medical Scientist Training Program (A.M.), the Canadian Institutes for Health Research (C.G.d.B.), the Charles A. King Trust Postdoctoral Research Fellowship Program, Bank of America, N.A., Co-Trustee, and the Simeon J. Fortin Charitable Foundation, Bank of America, N.A. (M.S.K.).

AUTHOR CONTRIBUTIONS

M.M., A.M., and D.B. designed the study with assistance from C.G.d.B. and M.S.K. M.M. conducted the experimental work with assistance from A.M., K.L., and P.H. M.S.K., N.R., A.R.K., D.F., M.M., A.M., P.H., and K.L. conducted bulk and scRNA-seq and sample perpetrations. C.G.d.B. performed the bioinformatics analysis. M.M., A.M., A.R., and D.B. wrote the manuscript with contributions from C.G.d.B. and M.S.K.

DECLARATION OF INTERESTS

The authors declare no competing interests.

Received: June 10, 2018
Revised: October 5, 2018
Accepted: November 13, 2018
Published: December 11, 2018

REFERENCES

Akunuru, S., and Geiger, H. (2016). Aging, clonality, and rejuvenation of hematopoietic stem cells. Trends Mol. Med. *22*, 701–712.

Amit, I., Garber, M., Chevrier, N., Leite, A.P., Donner, Y., Eisenhaure, T., Guttman, M., Grenier, J.K., Li, W., Zuk, O., et al. (2009). Unbiased reconstruction of a mammalian transcriptional network mediating pathogen responses. Science *326*, 257–263.

Baldridge, M.T., King, K.Y., Boles, N.C., Weksberg, D.C., and Goodell, M.A. (2010). Quiescent haematopoietic stem cells are activated by IFN-gamma in response to chronic infection. Nature *465*, 793–797.

Beerman, I., Bhattacharya, D., Zandi, S., Sigvardsson, M., Weissman, I.L., Bryder, D., and Rossi, D.J. (2010). Functionally distinct hematopoietic stem cells modulate hematopoietic lineage potential during aging by a mechanism of clonal expansion. Proc. Natl. Acad. Sci. USA *107*, 5465–5470.

Benz, C., Copley, M.R., Kent, D.G., Wohrer, S., Cortes, A., Aghaeepour, N., Ma, E., Mader, H., Rowe, K., Day, C., et al. (2012). Hematopoietic stem cell subtypes expand differentially during development and display distinct lymphopoietic programs. Cell Stem Cell *10*, 273–283.

Bernitz, J.M., Kim, H.S., MacArthur, B., Sieburg, H., and Moore, K. (2016). Hematopoietic stem cells count and remember self-renewal divisions. Cell *167*, 1296–1309.e10.

Bhatt, D.M., Pandya-Jones, A., Tong, A.-J., Barozzi, I., Lissner, M.M., Natoli, G., Black, D.L., and Smale, S.T. (2012). Transcript dynamics of proinflammatory genes revealed by sequence analysis of subcellular RNA fractions. Cell *150*, 279–290.

Cabezas-Wallscheid, N., Klimmeck, D., Hansson, J., Lipka, D.B., Reyes, A., Wang, Q., Weichenhan, D., Lier, A., von Paleske, L., Renders, S., et al. (2014). Identification of regulatory networks in HSCs and their immediate progeny via integrated proteome, transcriptome, and DNA methylome analysis. Cell Stem Cell *15*, 507–522.

Chung, N.C., and Storey, J.D. (2015). Statistical significance of variables driving systematic variation in high-dimensional data. Bioinformatics *31*, 545–554.

Colmegna, I., Diaz-Borjon, A., Fujii, H., Schaefer, L., Goronzy, J.J., and Weyand, C.M. (2008). Defective proliferative capacity and accelerated

telomeric loss of hematopoietic progenitor cells in rheumatoid arthritis. Arthritis Rheum. *58*, 990–1000.

Denkinger, M.D., Leins, H., Schirmbeck, R., Florian, M.C., and Geiger, H. (2015). HSC aging and senescent immune remodeling. Trends Immunol. *36*, 815–824.

Dykstra, B., Kent, D., Bowie, M., McCaffrey, L., Hamilton, M., Lyons, K., Lee, S.-J., Brinkman, R., and Eaves, C. (2007). Long-term propagation of distinct hematopoietic differentiation programs in vivo. Cell Stem Cell *1*, 218–229.

Dykstra, B., Olthof, S., Schreuder, J., Ritsema, M., and de Haan, G. (2011). Clonal analysis reveals multiple functional defects of aged murine hematopoietic stem cells. J. Exp. Med. *208*, 2691–2703.

Esplin, B.L., Shimazu, T., Welner, R.S., Garrett, K.P., Nie, L., Zhang, Q., Humphrey, M.B., Yang, Q., Borghesi, L.A., and Kincade, P.W. (2011). Chronic exposure to a TLR ligand injures hematopoietic stem cells. J. Immunol. *186*, 5367–5375.

Flach, J., Bakker, S.T., Mohrin, M., Conroy, P.C., Pietras, E.M., Reynaud, D., Alvarez, S., Diolaiti, M.E., Ugarte, F., Forsberg, E.C., et al. (2014). Replication stress is a potent driver of functional decline in ageing haematopoietic stem cells. Nature *512*, 198–202.

Geiger, H., de Haan, G., and Florian, M.C. (2013). The ageing haematopoietic stem cell compartment. Nat. Rev. Immunol. *13*, 376–389.

Gekas, C., and Graf, T. (2013). CD41 expression marks myeloid-biased adult hematopoietic stem cells and increases with age. Blood *121*, 4463–4472.

Granek, J.A., and Clarke, N.D. (2005). Explicit equilibrium modeling of transcription-factor binding and gene regulation. Genome Biol. *6*, R87.

Grover, A., Sanjuan-Pla, A., Thongjuea, S., Carrelha, J., Giustacchini, A., Gambardella, A., Macaulay, I., Mancini, E., Luis, T.C., Mead, A., et al. (2016). Single-cell RNA sequencing reveals molecular and functional platelet bias of aged haematopoietic stem cells. Nat. Commun. *7*, 11075.

Haas, S., Hansson, J., Klimmeck, D., Loeffler, D., Velten, L., Uckelmann, H., Wurzer, S., Prendergast, Á.M., Schnell, A., Hexel, K., et al. (2015). Inflammation-induced emergency megakaryopoiesis driven by hematopoietic stem cell-like megakaryocyte progenitors. Cell Stem Cell *17*, 422–434.

Hao, S., and Baltimore, D. (2009). The stability of mRNA influences the temporal order of the induction of genes encoding inflammatory molecules. Nat. Immunol. *10*, 281–288.

Jiang, J., Chan, Y.-S., Loh, Y.-H., Cai, J., Tong, G.-Q., Lim, C.-A., Robson, P., Zhong, S., and Ng, H.-H. (2008). A core Klf circuitry regulates self-renewal of embryonic stem cells. Nat. Cell Biol. *10*, 353–360.

Jovanovic, M., Rooney, M.S., Mertins, P., Przybylski, D., Chevrier, N., Satija, R., Rodriguez, E.H., Fields, A.P., Schwartz, S., Raychowdhury, R., et al. (2015). Immunogenetics. Dynamic profiling of the protein life cycle in response to pathogens. Science *347*, 1259038.

Kharchenko, P.V., Silberstein, L., and Scadden, D.T. (2014). Bayesian approach to single-cell differential expression analysis. Nat. Methods *11*, 740–742.

Khurana, S., Schouteden, S., Manesia, J.K., Santamaria-Martínez, A., Huelsken, J., Lacy-Hulbert, A., and Verfaillie, C.M. (2016). Outside-in integrin signalling regulates haematopoietic stem cell function via Periostin-Itgav axis. Nat. Commun. *7*, 13500.

King, K.Y., and Goodell, M.A. (2011). Inflammatory modulation of HSCs: viewing the HSC as a foundation for the immune response. Nat. Rev. Immunol. *11*, 685–692.

Kortylewski, M., Kujawski, M., Herrmann, A., Yang, C., Wang, L., Liu, Y., Salcedo, R., and Yu, H. (2009). Toll-like receptor 9 activation of signal transducer and activator of transcription 3 constrains its agonist-based immunotherapy. Cancer Res. *69*, 2497–2505.

Kovtonyuk, L.V., Fritsch, K., Feng, X., Manz, M.G., and Takizawa, H. (2016). Inflamm-aging of hematopoiesis, hematopoietic stem cells, and the bone marrow microenvironment. Front. Immunol. *7*, 502.

Kowalczyk, M.S., Tirosh, I., Heckl, D., Rao, T.N., Dixit, A., Haas, B.J., Schneider, R.K., Wagers, A.J., Ebert, B.L., and Regev, A. (2015). Single-cell RNA-seq reveals changes in cell cycle and differentiation programs upon aging of hematopoietic stem cells. Genome Res. *25*, 1860–1872.

Lara-Astiaso, D., Weiner, A., Lorenzo-Vivas, E., Zaretsky, I., Jaitin, D.A., David, E., Keren-Shaul, H., Mildner, A., Winter, D., Jung, S., et al. (2014). Immunogenetics. Chromatin state dynamics during blood formation. Science *345*, 943–949.

Li, B., and Dewey, C.N. (2011). RSEM: accurate transcript quantification from RNA-seq data with or without a reference genome. BMC Bioinformatics *12*, 323.

Mantel, C., Messina-Graham, S., Moh, A., Cooper, S., Hangoc, G., Fu, X.-Y., and Broxmeyer, H.E. (2012). Mouse hematopoietic cell-targeted STAT3 deletion: stem/progenitor cell defects, mitochondrial dysfunction, ROS overproduction, and a rapid aging-like phenotype. Blood *120*, 2589–2599.

Mayr, C., and Bartel, D.P. (2009). Widespread shortening of 3′UTRs by alternative cleavage and polyadenylation activates oncogenes in cancer cells. Cell *138*, 673–684.

McLean, C.Y., Bristor, D., Hiller, M., Clarke, S.L., Schaar, B.T., Lowe, C.B., Wenger, A.M., and Bejerano, G. (2010). GREAT improves functional interpretation of cis-regulatory regions. Nat. Biotechnol. *28*, 495–501.

Mehta, A., Zhao, J.L., Sinha, N., Marinov, G.K., Mann, M., Kowalczyk, M.S., Galimidi, R.P., Du, X., Erikci, E., Regev, A., et al. (2015). The microRNA-132 and microRNA-212 cluster regulates hematopoietic stem cell maintenance and survival with age by buffering FOXO3 expression. Immunity *42*, 1021–1032.

Morita, Y., Ema, H., and Nakauchi, H. (2010). Heterogeneity and hierarchy within the most primitive hematopoietic stem cell compartment. J. Exp. Med. *207*, 1173–1182.

Mossadegh-Keller, N., Sarrazin, S., Kandalla, P.K., Espinosa, L., Stanley, E.R., Nutt, S.L., Moore, J., and Sieweke, M.H. (2013). M-CSF instructs myeloid lineage fate in single haematopoietic stem cells. Nature *497*, 239–243.

Nagai, Y., Garrett, K.P., Ohta, S., Bahrun, U., Kouro, T., Akira, S., Takatsu, K., and Kincade, P.W. (2006). Toll-like receptors on hematopoietic progenitor cells stimulate innate immune system replenishment. Immunity *24*, 801–812.

Nemeth, J.A., Nakada, M.T., Trikha, M., Lang, Z., Gordon, M.S., Jayson, G.C., Corringham, R., Prabhakar, U., Davis, H.M., and Beckman, R.A. (2007). Alpha-v integrins as therapeutic targets in oncology. Cancer Invest. *25*, 632–646.

Ng, S.Y.-M., Yoshida, T., Zhang, J., and Georgopoulos, K. (2009). Genome-wide lineage-specific transcriptional networks underscore Ikaros-dependent lymphoid priming in hematopoietic stem cells. Immunity *30*, 493–507.

Novershtern, N., Subramanian, A., Lawton, L.N., Mak, R.H., Haining, W.N., McConkey, M.E., Habib, N., Yosef, N., Chang, C.Y., Shay, T., et al. (2011). Densely interconnected transcriptional circuits control cell states in human hematopoiesis. Cell *144*, 296–309.

O'Connell, R.M., Rao, D.S., Chaudhuri, A.A., Boldin, M.P., Taganov, K.D., Nicoll, J., Paquette, R.L., and Baltimore, D. (2008). Sustained expression of microRNA-155 in hematopoietic stem cells causes a myeloproliferative disorder. J. Exp. Med. *205*, 585–594.

O'Connell, R.M., Chaudhuri, A.A., Rao, D.S., Gibson, W.S., Balazs, A.B., and Baltimore, D. (2010). MicroRNAs enriched in hematopoietic stem cells differentially regulate long-term hematopoietic output. Proc. Natl. Acad. Sci. USA *107*, 14235–14240.

Pang, W.W., Price, E.A., Sahoo, D., Beerman, I., Maloney, W.J., Rossi, D.J., Schrier, S.L., and Weissman, I.L. (2011). Human bone marrow hematopoietic stem cells are increased in frequency and myeloid-biased with age. Proc. Natl. Acad. Sci. USA *108*, 20012–20017.

Picelli, S., Björklund, Å.K., Faridani, O.R., Sagasser, S., Winberg, G., and Sandberg, R. (2013). Smart-seq2 for sensitive full-length transcriptome profiling in single cells. Nat. Methods *10*, 1096–1098.

Pietras, E.M., Reynaud, D., Kang, Y.-A., Carlin, D., Calero-Nieto, F.J., Leavitt, A.D., Stuart, J.M., Göttgens, B., and Passegué, E. (2015). Functionally distinct subsets of lineage-biased multipotent progenitors control blood production in normal and regenerative conditions. Cell Stem Cell *17*, 35–46.

Ramirez-Carrozzi, V.R., Braas, D., Bhatt, D.M., Cheng, C.S., Hong, C., Doty, K.R., Black, J.C., Hoffmann, A., Carey, M., and Smale, S.T. (2009). A unifying model for the selective regulation of inducible transcription by CpG islands and nucleosome remodeling. Cell *138*, 114–128.

Robinson, M.D., McCarthy, D.J., and Smyth, G.K. (2010). edgeR: a Bioconductor package for differential expression analysis of digital gene expression data. Bioinformatics *26*, 139–140.

Rossi, D.J., Bryder, D., Zahn, J.M., Ahlenius, H., Sonu, R., Wagers, A.J., and Weissman, I.L. (2005). Cell intrinsic alterations underlie hematopoietic stem cell aging. Proc. Natl. Acad. Sci. U.S.A. *102*, 9194–9199.

Sanjuan-Pla, A., Macaulay, I.C., Jensen, C.T., Woll, P.S., Luis, T.C., Mead, A., Moore, S., Carella, C., Matsuoka, S., Bouriez Jones, T., et al. (2013). Platelet-biased stem cells reside at the apex of the haematopoietic stem-cell hierarchy. Nature *502*, 232–236.

Sawai, C.M., Babovic, S., Upadhaya, S., Knapp, D.J.H.F., Lavin, Y., Lau, C.M., Goloborodko, A., Feng, J., Fujisaki, J., Ding, L., et al. (2016). Hematopoietic stem cells are the major source of multilineage hematopoiesis in adult animals. Immunity *45*, 597–609.

Shahrin, N.H., Diakiw, S., Dent, L.A., Brown, A.L., and D'Andrea, R.J. (2016). Conditional knockout mice demonstrate function of Klf5 as a myeloid transcription factor. Blood *128*, 55–59.

Shattil, S.J., Kashiwagi, H., and Pampori, N. (1998). Integrin signaling: the platelet paradigm. Blood *91*, 2645–2657.

Sudo, K., Ema, H., Morita, Y., and Nakauchi, H. (2000). Age-associated characteristics of murine hematopoietic stem cells. J. Exp. Med. *192*, 1273–1280.

Sun, D., Luo, M., Jeong, M., Rodriguez, B., Xia, Z., Hannah, R., Wang, H., Le, T., Faull, K.F., Chen, R., et al. (2014). Epigenomic profiling of young and aged HSCs reveals concerted changes during aging that reinforce self-renewal. Cell Stem Cell *14*, 673–688.

Tanay, A., and Regev, A. (2017). Scaling single-cell genomics from phenomenology to mechanism. Nature *541*, 331–338.

Taniguchi Ishikawa, E., Chang, K.H., Nayak, R., Olsson, H.A., Ficker, A.M., Dunn, S.K., Madhu, M.N., Sengupta, A., Whitsett, J.A., Grimes, H.L., and Cancelas, J.A. (2013). Klf5 controls bone marrow homing of stem cells and progenitors through Rab5-mediated β1/β2-integrin trafficking. Nat. Commun. *4*, 1660.

Umemoto, T., Yamato, M., Shiratsuchi, Y., Terasawa, M., Yang, J., Nishida, K., Kobayashi, Y., and Okano, T. (2006). Expression of integrin beta3 is correlated to the properties of quiescent hemopoietic stem cells possessing the side population phenotype. J. Immunol. *177*, 7733–7739.

Umemoto, T., Yamato, M., Shiratsuchi, Y., Terasawa, M., Yang, J., Nishida, K., Kobayashi, Y., and Okano, T. (2008). CD61 enriches long-term repopulating hematopoietic stem cells. Biochem. Biophys. Res. Commun. *365*, 176–182.

Wagner, A., Regev, A., and Yosef, N. (2016). Revealing the vectors of cellular identity with single-cell genomics. Nat. Biotechnol. *34*, 1145–1160.

Wang, J., Sun, Q., Morita, Y., Jiang, H., Gross, A., Lechel, A., Hildner, K., Guachalla, L.M., Gompf, A., Hartmann, D., et al. (2012). A differentiation checkpoint limits hematopoietic stem cell self-renewal in response to DNA damage. Cell *148*, 1001–1014.

Weirauch, M.T., Yang, A., Albu, M., Cote, A.G., Montenegro-Montero, A., Drewe, P., Najafabadi, H.S., Lambert, S.A., Mann, I., Cook, K., et al. (2014). Determination and inference of eukaryotic transcription factor sequence specificity. Cell *158*, 1431–1443.

Wunder, E.W., and Henon, P.R. (2012). Peripheral Blood Stem Cell Autografts (Springer Science & Business Media).

Yamamoto, R., Morita, Y., Ooehara, J., Hamanaka, S., Onodera, M., Rudolph, K.L., Ema, H., and Nakauchi, H. (2013). Clonal analysis unveils self-renewing lineage-restricted progenitors generated directly from hematopoietic stem cells. Cell *154*, 1112–1126.

Yamamoto, R., Wilkinson, A.C., Ooehara, J., Lan, X., Lai, C.-Y., Nakauchi, Y., Pritchard, J.K., and Nakauchi, H. (2018). Large-Scale Clonal Analysis Resolves Aging of the Mouse Hematopoietic Stem Cell Compartment. Cell Stem Cell *22*, 600–607.e4.

Young, K., Borikar, S., Bell, R., Kuffler, L., Philip, V., and Trowbridge, J.J. (2016). Progressive alterations in multipotent hematopoietic progenitors underlie lymphoid cell loss in aging. J. Exp. Med. *213*, 2259–2267.

Yu, V.W.C., Yusuf, R.Z., Oki, T., Wu, J., Saez, B., Wang, X., Cook, C., Baryawno, N., Ziller, M.J., Lee, E., et al. (2016). Epigenetic memory underlies cell-autonomous heterogeneous behavior of hematopoietic stem cells. Cell *167*, 1310–1322.e17.

Zhao, J.L., Rao, D.S., Boldin, M.P., Taganov, K.D., O'Connell, R.M., and Baltimore, D. (2011). NF-kappaB dysregulation in microRNA-146a-deficient mice drives the development of myeloid malignancies. Proc. Natl. Acad. Sci. USA *108*, 9184–9189.

Zhao, J.L., Rao, D.S., O'Connell, R.M., Garcia-Flores, Y., and Baltimore, D. (2013). MicroRNA-146a acts as a guardian of the quality and longevity of hematopoietic stem cells in mice. eLife *2*, e00537.

Zhao, J.L., Ma, C., O'Connell, R.M., Mehta, A., DiLoreto, R., Heath, J.R., and Baltimore, D. (2014). Conversion of danger signals into cytokine signals by hematopoietic stem and progenitor cells for regulation of stress-induced hematopoiesis. Cell Stem Cell *14*, 445–459.

STAR★METHODS

KEY RESOURCES TABLE

REAGENT or RESOURCE	SOURCE	IDENTIFIER
Antibodies		
CD11c	Biolegend	117304 N418
CD3e	Biolegend	100304 145-2C11
NK1.1	Biolegend	108704 PK136
IL-7Ra	Biolegend	135006 A7R34
Ter-119	Biolegend	116204 TER-119
CD11b	Biolegend	101204 M1/70
CD8a	Biolegend	100704 53-6.7
CD4	eBioscience	13-0041-82 gk1.5
B220	Biolegend	103204 RA3-6B2
CD19	Biolegend	115504 6D5
GR-1	Biolegend	108403 RB6-8C5
CD45.1 PE	Biolegend	110708 a20
CD45.2 eflour 450	eBioscience	48-0454-82 104
GR1 APC	Biolegend	108412 RB6-8C5
CD3E FITC	Biolegend	100306 145-2C11
CD11B PE/CY5	Biolegend	101209 M1/70
CD45.2 PE/CY5	Biolegend	25-0454-80 104
CD3E PE/CY5	eBioscience	100310 145-2C11
IL-7Ra PE/CY5	Biolegend	135016 A7R34
NK1.1 PE/CY5	Biolegend	108716 PK136
GR1 PE/CY5	Biolegend	108410 RB6-8C5
cd11B PE/CY5	Biolegend	101209 M1/70
CD19 PE/CY5	Biolegend	115510 6D5
CD4 PE/CY5	BIolegend	15-0041-82 GK1.5
TER-119 PE/CY5	EBioscience	116209 TER-119
FC BLOCK	Biolegend	101302 93
CD150 PE/CY7	Biolegend	115914 TC15-12F12.2
CD45.2 APC/CY7	Biolegend	109824 104
CD34 EFLOUR450	Biolegend	48-0341-80 RAM34
CD34 PE	EBioscience	128610 HM34
IL-7Ra PE	Biolegend	135009 A7R34
CD48 PACBLUE	Biolegend	103418 HM48-1
CD61 PE	Biolegend	12-0611-82 2C9.G3
CD38 APC/CY7	EBioscience	102728 90
CD34 APC/CY7	BIolegend	128614 HM34
CD16/32 EFLOUR450	Biolegend	48-0161-82 93
CD16/32 VIOLET 420	EBioscience	101331 93
CD16/32 PE/CY7	Biolegend	25-0161-81 93
SCA1 APC	EBioscience	108112 D7
SCA1 PACBLUE	Biolegend	108120 D7
CKIT APC	Biolegend	105812 2B8
CKIT PE	Biolegend	1335106 ACK2

(*Continued on next page*)

Continued

REAGENT or RESOURCE	SOURCE	IDENTIFIER
CKIT FITC	Biolegend	105806 2B8
CD135 APC	Biolegend	135310 A2F10
CD41 PE	Biolegend	133906 B203323
CD51 PE	Biolegend	104106 B240646
CD61 APC	Biolegend	104316 B219725
Bacterial and Virus Strains		
PCL-ecotropic pseudotyped gamma-retrovirus	O'Connell et al., 2008	Adgene: #26528
Chemicals, Peptides, and Recombinant Proteins		
LPS	SIGMA	L2880-100MG
Pam3CSK4	Invivogen	41-11-60-10
Dulbecco's Modification of Eagle's Medium	Corning	10-013-CV
Fetal Bovine Serum	Corning	35-015-CV
Penicillin Streptomycin Solution (100x)	Corning	30-002-CI
0.25% Trypsin	Corning	25-053-CI
TRIzol Reagent	Invitrogen	15596026
Protoscript II	New England Biolabs	M0368L
Antarctic phosphatase	New England Biolabs	M0289S
Puromycin	InvivoGen	Cat#ant-pr-1
Murine SCF	PeproTech	250-03
Murine IL-6	PeproTech	216-16
Murine IL-3	PeproTech	213-13
Critical Commercial Assays		
BioT	Bioland	B01-01
Nextera XT DNA Library Preparation Kit	illumina	FC-131-1096
qScript cDNA SuperMix	Quanta	95048-100
KAPA HiFi HotStart ReadyMix	KAPA biosystems	KM2602
Deposited Data		
RNA-Seq Gene Expression and IR Data	This Paper	GEO: GSE100428
Experimental Models: Cell Lines		
HEK293T	ATCC	CRL-3216
Experimental Models: Organisms/Strains		
Mouse: C57BL/6J	Jackson Laboratory	000664
Mouse: C57BL/6J	Charles Rivers Laboratories	C57BL/6NCrl
Oligonucleotides - source		
Primers used	Table S5	This paper
shRNA sequences	Table S5	This paper
cDNA sequences for TFs overexpression	Table S5	This paper

CONTACT FOR REAGENT AND RESOURCE SHARING

Further information and requests for resources and reagents should be directed to and will be fulfilled by the Lead Contact, Mati Mann (mati@caltech.edu).

EXPERIMENTAL MODEL AND SUBJECT DETAILS

Mice

The California Institute of Technology Institutional Animal Care and Use Committee approved all experiments. Young and aged C57BL/6 WT males and females mice were obtained from Charles Rivers Laboratories and housed in the Caltech Office of Laboratory Animal Resources (OLAR) facility. For all experiments, young mice were between 8-12 weeks of age and aged mice were between 20-24 months of age.

METHOD DETAILS

Flow cytometry

Tissues were first harvested and cells were homogenized. Samples were depleted of RBCs using RBC lysis buffer (BioLegend). Cells were subsequently stained with fluorescently labeled antibody. Respective cell types were analyzed according to relevant surface markers by using the following antibodies: CD45.1 and CD45.2, lineage-specific markers (CD11b, Gr-1, CD19, B220, CD3e, Nk1.1 and Ter119), or progenitor-specific markers (CD150, CD48, Flt3, CD34, FcRgamma and IL7R). All antibodies were purchased from BioLegend. HSPCs were sorted by first lineage-depleting whole bone marrow from young and aged mice. Samples were incubated with biotin-conjugated lineage antibodies (CD19, B220, CD4, CD8, CD11b, Gr-1, Ter119, Nk1.1, IL7Ra each at 1:200 dilution), and passaged through Miltenyi MACS negative selection columns. Cells were subsequently analyzed with a MACSQuant10 Flow Cytometry machine (Miltenyi), or sorted using BD Aria sorter. HSPCs were sorted using SLAM markers with the following gating strategies: for MPPs: Lineage-cKit+Sca1+CD150-CD48+, for ST-HSCs: Lineage-cKit+Sca1+CD150-CD48- and for LT-HSCs: Lineage-cKit+Sca1+CD150+CD48-, with or without CD61. Gating strategies for other cell types used in our analysis are described in Figure S8. (Complete list of antibodies catalog numbers and lots can be found in Key Resources Table)

Cell culture

Cells were cultured in a sterile incubator that was maintained at 37°C and 5% CO_2. Primary cells were cultured in HSPC media, comprised of complete RPMI supplemented with 10% FBS, 100 U/mL penicillin, 100 U/mL streptomycin, 50uM β-mercaptoethanol and mouse SCF (50 ng/mL), IL-3 (20 ng/mL), and IL-6 (50 ng/mL) when cultured for reconstitution experiments. 293T cells were cultured in DMEM supplemented with 10% fetal bovine serum, 100 U/mL penicillin and 100 U/mL streptomycin. For *in vitro* stimulation, sorted HSPCs were incubated in HSPC media with 100ng/ml LPS (SIGMA CAT: L2880-100MG), and 1ug/ml Pam3csk4 (Invivogen CAT: 41-11-60-10) for the indicated time points.

Bone marrow transplant experiments

Bone marrow reconstitution experiments were performed using aged and young unmanipulated cells or with the vectors noted below. Aged and young WT CD45.2 C57BL/6 mice were treated with 5-fluorouracil (10ug; Sigma) for 5 days to enrich for hematopoietic stem and progenitor cells (HSPCs) in the bone marrow. After 5 days, bone marrow cells were harvested, red blood cells (RBCs) were lysed with RBC lysis buffer (BioLegend), and cells were plated in HSPC media (see above). Cells were then cultured for 24 hours and spin-infected for 2 hours at 30°C and 2500RPM with PCL-ecotropic pseudotyped gamma-retrovirus expressing the shRNA or cDNA of interest (see Key Resources table). Virus supernatant was then removed and replaced with HSPC media. A second round of spin infection was performed 24 hours later. 24hrs after the last infection, recipient mice were lethally irradiated (1000 rads) and 250,000 virus-infected HSPCs were retro-orbitally delivered to reconstitute the immune system.

Recipient mice were monitored for health and peripheral blood was analyzed for mature blood cell types every 4 weeks or at 4 hours after each LPS injection up till secondary transplant, or till the experimental endpoint 16 weeks post-reconstitution. At each endpoint, immune organs were harvested for further analysis. The number of mice for each experimental cohort is described in the figure legends.

For LT-HSC, ST-HSC or MPPs, from either young or aged CD45.2 mice, donor bone marrow was extracted and lineage depleted cells were sorted for each cell population (see sorting procedure above). Cells were then processed for transplant or stimulated with LPS and Pam3csk4 as described above for 2 hours prior to transplantation. A total of 1000 sorted cells were injected together with 100,000 supporting CD45.1 bone marrow cells from young donors into irradiated young CD45.1 recipient mice. For secondary transplant experiments, 250,000-500,000 cells from whole bone marrow of primary transplant mice were transplanted into irradiated young CD45.1 recipient mice. For CD61 reconstitution experiments, 100 CD61 high or CD61 low LT-HSCs from young or aged CD45.2 mice were injected into irradiated young CD45.1 mice together with 200,000 supporting total bone marrow cells from young CD45.1 mice. Each experiment was repeated at least twice, and in many cases three times.

In vivo LPS challenge

Mice were injected intraperitoneally with a sublethal dose of LPS (0.5ug/gram, SIGMA CAT: L2880-100MG), and were bled before injections, and after 24hrs, 7days, 14days and 7 weeks. Blood samples were analyzed for CD11b, CD3e, CD19, and Gr1 expressing cells to asses mature immune cell populations. In some cases, a secondary injection of 0.5ug/gram LPS was conducted followed by immune cell repertoire in peripheral blood as with the first injection. For chronic LPS injections, mice were injected with 0.1ug/gram twice weekly for 12weeks. Mice were then harvested, blood samples were analyzed for CD11b, CD3e, CD19, and Gr1 expressing cells to asses mature immune cell populations, and bone marrow cells were analyzed for LT-HSC, ST-HSC, MPP as well as CD61 on LT-HSCs.

Bulk RNA-seq

For bulk RNA-seq, LT-HSCs, ST-HSCs and MPPs from aged and young mice were sorted as described above. Cells were then stimulated *in vitro* for 0.5, 1hr, 2hr, 4hr, 8hr, or 12hr with 100ng/ml LPS (SIGMA CAT: L2880-100MG), and 1ug/ml Pam3CSK4 (Invivogen CAT: 41-11-60-10). mRNA extraction was performed using the PrepEase RNA Spin Kit (usb®). RNA quality was assessed

using RNA 6000 Pico Kit (Agilent). Full-length RNA-seq libraries were prepared as previously described (Kowalczyk et al., 2015) and paired-end sequenced (38bp x 2) on an Illumina HiSeq2500.

scRNA-seq

For full-length scRNA-seq, LT-HSCs, ST-HSCs and MPPs from aged and young mice were sorted as described above and stimulated *in vitro* for 2 hours in large volumes (2000-3000 cells in 10mL of media) to minimize secondary stimulation with secreted cytokines. Single cells were subsequently sorted into 96 well plates containing 5ul TCL Buffer (QIAGEN) with 1% 2-mercaptoethanol, centrifuged and frozen at −80°C. SMART-Seq2 protocol was carried out as previously described (Picelli et al., 2013) with minor modifications (M.S.K. and A.R., unpublished data). cDNA was amplified with 20 cycles and tagmented with a quarter of the standard Illumina NexteraXT reaction volume. Single-cell libraries were pooled and paired-end sequenced (38bp x 2) on an Illumina Hiseq2500 or Nextseq500.

DNA constructs

For *in vivo* Ikzf1, Klf4, Klf5, Hoxa9, Zbtb4, Stat3 shRNA experiments, the mature shRNA sequence was synthesized in the microRNA-155 loop-and-arms format (O'Connell et al., 2010) and cloned into the MSCV-eGFP (MG). All shRNA sequences are provided in Reagents and Resources. For overexpression of *Ikzf1*, *Klf5*, and *Stat3*, the cDNA of each TF was cloned into a PIG vector (Mayr and Bartel, 2009) (Addgene plasmid # 21654). All cDNA sequences cloned are provided in Table S5. Virus production is described below.

Virus production

To generate retrovirus for HSPC infection, 10^6 HEK293T cells were first plated in a 15cm plate. 24 hours later, cells were transfected with both the pCL-Eco vector and either the MG or PIG vector with the relevant shRNA or cDNA described above for gene delivery. For transfection, we used BioT (Bioland Scientific) as per the manufacturer's protocol. 36 hours after transfection, virus was collected, filtered through a 45uM syringe filter, and used for infection of HSPCs.

QUANTIFICATION AND STATISTICAL ANALYSIS

Bulk RNA-seq analysis

RNA-seq reads for both single cell and bulk were aligned to the mm9 UCSC transcriptome and quantified using RSEM (Bowtie versions 1.27 and 0.12.7, respectively) (Li and Dewey, 2011). Gene-level counts were TMM-normalized and edgeR (Robinson et al., 2010) was used to call differentially expressed genes, comparing each time point to time 0, for all cell types and mouse ages. We also considered baseline differences between cell types and mouse ages. P values were adjusted for multiple hypothesis testing by Benjamini-Hochberg FDR correction, with FDR < 0.01 considered for subsequent analysis.

Single cell RNA-seq analysis

Cells that had fewer than 2000 genes detected, a lower than 25% rate of reads mapping to the transcriptome, or were undergoing the cell cycle (Kowalczyk et al., 2015) were excluded from analysis. We also excluded outlier cells from the MPPs group which were likely caused by cell contamination. To correct for batch issues, the two experimental batches were centered to have the same mean log(TP100K+1) (hereafter referred to as log(TPM), where TPM stands for 'transcripts per million') per gene. PCA was done in R with scaled, centered log(TPM), using only genes annotated with GO terms we considered important in our system, including cytokine receptor binding, immune system development, immune system process, inflammatory response, response to cytokine, single-organism developmental process, stem cell, cell proliferation, and autophagy. The permutationPA function from jackstraw (Chung and Storey, 2015) was used to select significant PCs and then tSNE (tSNE package, with default parameters) was used to reduce the data to two dimensions. Density-based clustering was performed (package dbscan, eps = 5, minPts = 20) and the resulting three clusters were used for subsequent analysis.

Single-cell differential expression and gene signatures

All single-cell differential expression analysis was performed with single cell differential expression (SCDE) (Kharchenko et al., 2014), considering only genes that had at least 50 reads and were detected in at least 5 cells. For all signatures, a cell's signature score is the weighted sum of log(TPM) of genes, weighted by the direction of the enrichment (either +1 for enriched genes or −1 for depleted genes).

Stimulated mLT-HSC signature

Genes with a DE FDR < 0.1 when comparing stimulated LT-HSCs in cluster 3 to cluster 2 were defined as the signature of stimulated myeloid-biased LT-HSCs.

Unstimulated mLT-HSC signature

Genes where bulk RNA-seq data indicated a significant difference (FDR < 0.01) in expression between both aged versus young unstimulated LT-HSCs, and between cluster 3 versus cluster 2 LT-HSCs (in the same direction) were used as an initial estimate of a

common mLT-HSC signature. Next, a weighted sum of the genes in this common signature was used to score each of the unstimulated LT-HSCs, and the cells were partitioned into two groups on this basis. The centroids of these two groups of cells were used to initialize *k*-means clustering ($k = 2$) of the unstimulated LT-HSCs, performed in PC-space with PCs 2-10 of a PCA of all expressed genes in unstimulated LT-HSCs only (PC1 was correlated with batch, and so was excluded here). This yielded two new clusters, similar but distinct from those with which we initialized the k-means clustering algorithm. SCDE was used to identify differentially expressed genes (FDR < 0.1) between the cells in these two clusters (representing myeloid-biased and non-myeloid-biased unstimulated LTs), yielding an unstimulated myeloid-biased LT signature.

TF motif analysis

Enhancers from diverse mouse blood cells (Lara-Astiaso et al., 2014) were associated with neighboring genes with GREAT (McLean et al., 2010) and each was scanned for the mouse and (when mouse was not available) human TF motifs from CIS-BP (Weirauch et al., 2014) using an implementation of GOMER (Granek and Clarke, 2005), yielding a TF binding score for each TF/enhancer pair. TFs that distinguish cell subsets were defined as those that best discriminate between enhancers associated with genes that are specific to the subset compared to enhancers that are associated with non-specific, but expressed genes using the Wilcoxon rank sum test, yielding an enrichment score (AUROC) and P value. P values were subsequently corrected for multiple hypothesis testing with FDR correction, considering only those with FDR < 0.1 for subsequent analysis.

Statistical tests

All statistical analysis for the phenotypic data was done in Graphpad Prism software using an unpaired Student's t test, or a 1-way or 2-way ANOVA. Data is reported as mean ± SEM (statistical test is depicted in each figure legend). Significance measurements were marked as follows: * $p < 0.05$, ** $p < 0.01$, *** $p < 0.001$, or ns for not significant. P values were corrected for multiple hypothesis testing by Bonferroni's multiple comparison test.

Replicate information is indicated in the figure legends.

DATA AND SOFTWARE AVAILABILITY

The accession number for the sequencing data in this paper is GEO: GSE100428.